Karlsruhe Institute of Technology

Who Adopts Where and When? Electric Vehicle Diffusion with Building-Level Localization in Germany

Moritz Raab, Max Kleinebrahm, Jonathan Vogl, Tim Signer, Jannik Braun, and Wolf Fichtner IIP, KIT

No. 82| AUGUST 2026

WORKING PAPER SERIES IN PRODUCTION AND ENERGY

Who Adopts Where and When? Electric Vehicle Diffusion with Building-Level Localization in Germany

Moritz Raab, Max Kleinebrahm, Jonathan Vogl, Tim Signer, Jannik Braun, and Wolf Fichtner IIP, KIT

(Contact) Chair of Energy Economics, Institute for Industrial Production
(IIP) at the Karlsruhe Institute of Technology (KIT),
Hertzstr. 16, buliding 06.33, 76187 Karlsruhe,
Tel. +49 721 608- 44468, email: moritz.raab@kit.edu

Abstract:

The electrification of private vehicles is a central element of decarbonizing transport and energy systems. Accurately anticipating when and where electric vehicles will be adopted is critical for charging infrastructure planning, distribution grid planning, and energy system operation, yet most diffusion models represent adoption at aggregated spatial scales. Here we introduce an open, high-resolution technology diffusion framework that links household-level electric vehicle adoption with GPS-exact residential locations. The framework combines a synthetic population, household-to-building matching, car ownership modeling, and a national Bass diffusion trajectory to translate aggregate electric vehicle growth into localized adoption pathways. We apply the framework to Germany from 2025 to 2050 and validate its main components against Census marginals, building assignments, and registered vehicle counts, demonstrating its suitability for spatially explicit EV diffusion analysis. The results reveal substantial spatial heterogeneity in electric vehicle diffusion across regions, municipalities, grid cells, and buildings. Differences in household income and the share of single-family houses shape local adoption trajectories, leading to higher adoption in West Germany than in East Germany and slightly higher adoption in rural than urban municipalities in aggregate. The framework provides an open and transferable basis for spatially explicit modeling of household technology adoption. Future research can build on these findings by applying the framework to other technologies or by linking GPS-exact electric vehicle diffusion to charging demand, system operation, and infrastructure planning

Highlights

Who Adopts Where and When? Electric Vehicle Diffusion with Building-Level Localization in Germany

Moritz Raab, Max Kleinebrahm, Jonathan Vogl, Tim Signer, Jannik Braun, Wolf Fichtner

- GPS-exact electric vehicle diffusion is modeled for Germany.
- Technology adoption is linked to household sociodemographic characteristics.
- Electric vehicle diffusion shows strong spatial heterogeneity.
- Building-level results reveal local patterns hidden by aggregation.
- Open, transferable framework for spatial technology diffusion modeling.

Who Adopts Where and When? Electric Vehicle Diffusion with Building-Level Localization in Germany

Moritz Raab[a], Max Kleinebrahm[a], Jonathan Vogl[a], Tim Signer[a], Jannik Braun[a] and Wolf Fichtner[a]

[a] Institute for Industrial Production, Karlsruhe Institute for Technology (KIT), Hertzstr. 16, Karlsruhe, 76187, Germany

ARTICLE INFO

Keywords:
Technology diffusion
Electric vehicle adoption
Synthetic population
Spatially explicit modeling
Household-level adoption
Building-level modeling

ABSTRACT

The electrification of private vehicles is a central element of decarbonizing transport and energy systems. Accurately anticipating when and where electric vehicles will be adopted is critical for charging infrastructure planning, distribution grid planning, and energy system operation, yet most diffusion models represent adoption at aggregated spatial scales. Here we introduce an open, high-resolution technology diffusion framework that links household-level electric vehicle adoption with GPS-exact residential locations. The framework combines a synthetic population, household-to-building matching, car ownership modeling, and a national Bass diffusion trajectory to translate aggregate electric vehicle growth into localized adoption pathways. We apply the framework to Germany from 2025 to 2050 and validate its main components against Census marginals, building assignments, and registered vehicle counts, demonstrating its suitability for spatially explicit EV diffusion analysis. The results reveal substantial spatial heterogeneity in electric vehicle diffusion across regions, municipalities, grid cells, and buildings. Differences in household income and the share of single-family houses shape local adoption trajectories, leading to higher adoption in West Germany than in East Germany and slightly higher adoption in rural than urban municipalities in aggregate. The framework provides an open and transferable basis for spatially explicit modeling of household technology adoption. Future research can build on these findings by applying the framework to other technologies or by linking GPS-exact electric vehicle diffusion to charging demand, system operation, and infrastructure planning.

1. Introduction

In 2024, global electric vehicle (EV) sales climbed to a record 17 million units, an increase of 25% compared with 2023 [1]. This growth is expected to persist, with the global EV fleet projected to expand from about 58 million vehicles in 2024 to around 235 million by 2030 [2]. While this rapid deployment substantially contributes to transport decarbonization, it simultaneously poses challenges to distribution grid infrastructure [3–5], including potential overloads occurring before transformers reach their capacity limit [6–8].

At the same time, EVs can provide flexibility services through controlled charging [9, 10]. Thereby, EVs can contribute to peak shaving, voltage and frequency regulation [11, 12], grid resilience, reduced requirements for stationary battery storage and costly grid reinforcements [13, 14], and facilitate the integration of renewable energy [15–19]. However, realizing these potentials requires an appropriate integration of EVs into the local energy system.

Consequently, regional planners and distribution system operators require spatial and temporal visibility into the evolution of electric vehicle adoption to ensure adequate system sizing and operation. More broadly, the same need for high-resolution adoption modeling applies to other distributed technologies such as heat pumps and rooftop photovoltaic systems, whose uptake and operation likewise shape local electricity demand and flexibility.

To our knowledge, no model currently exists that represents EV adoption at the household level with GPS-exact spatial localization while simultaneously accounting for sociodemographic determinants (Table 1). Mascherbauer et al. (2025) [20] model EV adoption at GPS-exact spatial resolution, however, EV allocation is not driven by household-specific sociodemographic adoption likelihoods. As a result, the interaction between household characteristics, residential location, and technology adoption remains insufficiently represented in the literature.

This limitation is particularly relevant at the distribution grid level, where overloads may be triggered by a small number of households with coincident charging peaks. While aggregation at the transformer or municipal level smooths these peaks, GPS-exact resolution reveals localized stress patterns that are crucial for grid planning (see Figure 1).

To address this gap, we develop a high-resolution technology diffusion model that integrates temporal (annual), spatial (GPS-exact), sociodemographic (e.g., household income), and residential dimensions (e.g., residential building type) within a unified framework. The framework combines three components: (i) the generation of a synthetic population calibrated to multi-level spatial marginals; (ii) the assignment of synthetic households to georeferenced buildings; and (iii) a hybrid diffusion-adoption module that links macroscopic diffusion dynamics with household-level adoption probabilities derived from observed adoption determinants. We demonstrate the framework in a case study of EV diffusion in Germany.

*Corresponding author
moritz.raab@kit.edu (M. Raab)
ORCID(s): 0009-0007-2563-9424 (M. Raab); 0000-0002-6957-2379 (M. Kleinebrahm); 0009-0007-5396-2085 (J. Vogl)

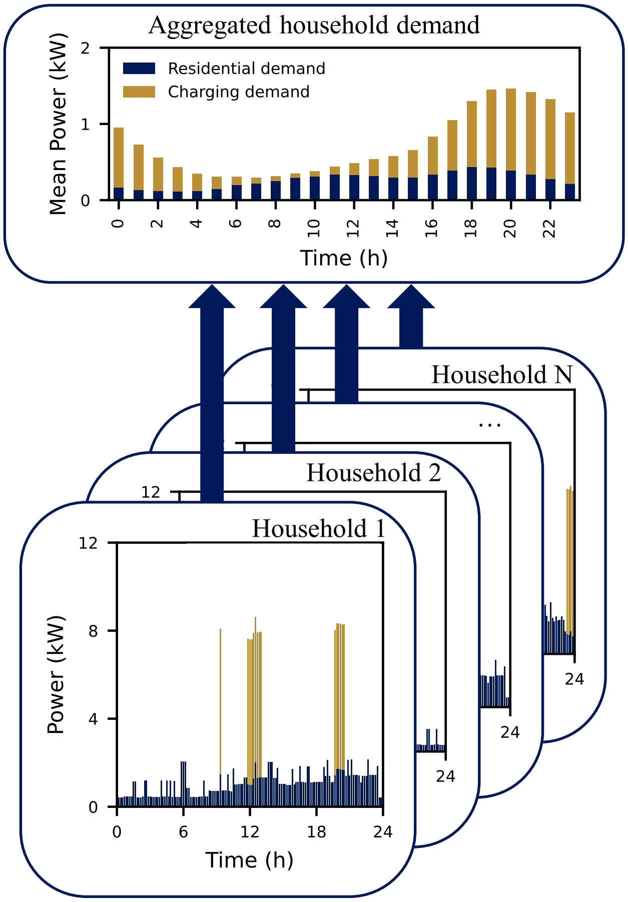

Fig. 1: Smoothing effect through spatial aggregation. The lower panel shows exemplary single-household load profiles with pronounced EV charging peaks relative to baseline residential demand, whereas the upper panel shows an aggregated profile for the average German household, in which charging peaks are substantially attenuated. This illustrates how GPS-exact, household-level resolution can reveal localized stress patterns that may be relevant for line overloads. Household profiles are based on [3, 21, 22], and the average German household profile is based on [23, 24].

By integrating sociodemographic heterogeneity with building-level spatial localization, the proposed model enables a differentiated analysis of EV adoption dynamics at distribution-grid-relevant scales. It thereby provides a foundation for improved assessment of localized grid impacts and flexibility potentials at the lowest spatial level. At the same time, the household-level sociodemographic resolution allows adoption patterns to be linked to questions of charging infrastructure access, energy poverty, and distributional equity in the diffusion of low-carbon technologies.

The remainder of this paper is structured as follows. Section 2 provides a literature overview. Section 3 and Section 4 describe the methodology and data. The results are presented in Section 5 and discussed in Section 6. In Section 7, conclusions are drawn, and an outlook is provided.

2. Literature review

The electrification of mobility and heating, together with the expansion of residential photovoltaics, increasingly reshapes electricity demand and generation at the low-voltage level, where detailed grids are often highly heterogeneous [32, 33]. The impact of technology deployment depends strongly on local grid characteristics, building stock, and the spatial concentration of new electricity demand [7, 34]. Geographically disaggregated analyses show that network upgrade costs and the value of flexibility can vary substantially between local areas, indicating that targeted flexibility deployment may reduce reinforcement needs more effectively than untargeted approaches [34]. Complementary studies of German low-voltage grids show that electric vehicles, heat pumps, and photovoltaics jointly affect transformer loading and that local coordination of flexible demand can mitigate distribution-grid constraints [7, 33]. These findings imply that distribution grid and local energy system analyses require adoption scenarios that are not only temporally resolved, but also spatially explicit at the level where loads and generation emerge.

However, existing demand-side analyses often rely on aggregated technology deployment assumptions [28, 34]. More broadly, technology adoption and diffusion models increasingly account for spatial [31, 35–40], temporal [35–42], and sociodemographic heterogeneity [31, 36–38, 40–42] through agent-based models [36–38], machine-learning methods [38–40], econometric models [31], and household-level adoption and use models for residential cooling technologies [41, 42]. Yet these approaches typically operate at aggregated spatial units, such as regions and grid cells, or use building agents that do not represent the sociodemographic composition of resident households. In the EV context, adoption and diffusion models likewise tend to represent adoption at aggregated spatial levels or estimate sociodemographic determinants without linking households to exact residential buildings [25, 27, 31]. As summarized in Table 1, no existing approach combines GPS-exact building-level localization with sociodemographic determinants of EV adoption. Addressing this gap requires integrating three methodological strands: synthetic population generation, spatial matching of households to buildings, and EV adoption modeling.

Synthetic population. Agent-based models commonly rely on synthetic population data representing households and individuals with attributes that drive behavioral decisions. The goal of synthetic reconstruction is to generate a population whose sociodemographic characteristics exhibit statistical distributions consistent with those of the real population. This includes capturing heterogeneity of households and individuals across geographic areas and reflecting interdependencies among members of the same household [43, 44]. The current state-of-the-art approach is Iterative Proportional Updating (IPU), which assigns weights to households from a representative microdata sample such that the weighted population matches known aggregate control totals

Table 1
Overview of spatio-temporal EV diffusion and adoption models. Studies are compared by temporal and spatial resolution, diffusion and adoption modeling approach, inclusion of sociodemographic determinants, adoption data source, and sample size. The final row summarizes the contribution of this work for direct comparison.

First author and year	Temporal resolution	Spatial resolution	Diffusion	Adoption	Sociodemographics	Adoption data	Size
Ensslen 2019 [25]	Yearly	✗	Bass	Logit regression	✓	Mobility Survey 2016	171
Cao Van 2023 [26]	Yearly	✗	ALADIN	✗	✗	Mobility Survey 2023	17k
Sica 2025 [27]	✗	✗	✗	Discrete choice	✓	Mobility Survey 2023	17k
Arnold 2024 [28]	Yearly	NUTS3	Bass	✗	✗		
Paevere 2014 [29]	Quarterly	LAU	✗	Multi criteria decision	✓	Mobility Survey 2011	2k
Heymann 2017 [30]	✗	LAU	✗	Multi linear regression	✓	Mobility Survey 2016	30
Sheng 2022 [31]	Yearly	LAU	✗	Binomial regression	✓	National Statistics 2020	
Mascherbauer 2025 [20]	Yearly	GPS-exact	✗	Random	✗		
This work	**Yearly**	**GPS-exact**	**Bass**	**Logit regression**	✓	**Mobility in Germany 2023**	**420k**

NUTS3: regional district level, LAU: municipal level

[43, 45]. IPU extends the Iterative Proportional Fitting algorithm [46] by calibrating household- and individual-level features simultaneously. The algorithm therefore relies on a representative microdata sample and on aggregated marginal distributions of household and individual features. Because relevant control variables may not be available at the same spatial resolution, extensions of IPU have been developed to calibrate synthetic populations to controls at multiple spatial resolutions, commonly referred to as multilevel IPU [47, 48].

In this paper, we use a two-level IPU procedure that calibrates household weights to German Census controls at both the municipal level and the 100×100 m grid-cell level. This is necessary because variables relevant for EV adoption are distributed across both spatial levels and must therefore be combined to construct a consistent synthetic population (see Section 4). The resulting population represents individual households as decision makers and provides the bottom-up basis for linking household-level adoption behavior to spatially resolved EV diffusion and its higher-level system implications. Related energy-system studies use similar approaches. For example, Kleinebrahm et al. apply iterative proportional fitting to generate a synthetic European building stock at the NUTS3 level and assess self-sufficient energy supply for single-family buildings across Europe [49].

Household-to-building matching. To enable geographically explicit analyses, synthetic households must be assigned to physical, georeferenced buildings. Such linkage is particularly relevant in transport modeling, as residential location influences individual mobility behavior and travel demand [50, 51]. This linkage is also relevant for energy system applications, for example, when analyzing EV charging, building electrification through heat pumps, or local load patterns, where coupling households with building-specific attributes such as construction age or dwelling size is essential.

Assigning synthetic households to buildings can be formulated as a generalized assignment problem, in which households are allocated to suitable residential buildings under compatibility and capacity constraints. Related studies in spatial microsimulation and urban modeling have addressed this problem through probabilistic or rule-based allocation procedures. Antoni et al. [52] generate synthetic households from aggregated sociodemographic and geographic data for French cities and subsequently assign them to buildings to create a population database for multi-agent and activity-based urban models. Thomson et al. [53] simulate geolocated synthetic households in Namibia by classifying household types and linking them to building coordinates using probability surfaces estimated from spatial covariates. These studies demonstrate the relevance of household-building linkage for spatial population modeling, but their assignment procedures are primarily designed for demographic, survey, or urban modeling applications rather than for allocating technology adoption and energy demand to individual buildings.

In this paper, we build on this idea and assign households to buildings using an optimization-based matching procedure that minimizes unused living area and can additionally account for building attributes such as construction age and building type. Compared with probabilistic allocation, this approach provides an optimal or near-optimal assignment with respect to the specified constraints. This is particularly important for building-level technology diffusion, because adoption-relevant household characteristics must be linked to plausible residential building attributes. For example, residential building type can affect the suitability for private EV charging and rooftop photovoltaics, while construction age and dwelling size are relevant for heating demand and heat pump adoption. An optimization-based assignment therefore reduces implausible household-building combinations and improves the consistency of localized adoption and demand estimates. The main trade-offs are higher computational effort and the possibility of leaving households unmatched when hard building-capacity constraints prevent feasible assignments.

EV adoption and diffusion. EV adoption is shaped by heterogeneous household, individual, and spatial characteristics. Previous studies show that adoption is associated with sociodemographic factors such as income, education, age, gender, and household size [54–59], as well as with behavioral and attitudinal factors including environmental concern and innovation affinity [54, 55, 60]. Spatial context also matters, as adoption patterns differ by region type and can be reinforced by neighborhood effects [54, 58, 59]. These findings motivate models that represent individual households as decision makers and link their characteristics to spatially explicit adoption probabilities.

In the literature, adoption models explain which households, individuals, or vehicle users are more likely to choose an electric vehicle, whereas diffusion models describe how EV uptake develops over time at the fleet or market level (see Table 1). Existing EV modeling approaches can be grouped into bottom-up, top-down, and hybrid approaches. Bottom-up approaches model adoption or vehicle choice at the household, individual, vehicle-user, or driving-profile level. They include adoption models based on regression [25, 30, 31] or discrete choice [27, 29], as well as techno-economic diffusion models such as ALADIN, which represents drivetrain choice based on driving profiles, total cost of ownership, infrastructure availability, and utility-based purchase decisions [26]. Top-down approaches instead project aggregate fleet growth using diffusion models such as the Bass model [25, 28]. Hybrid approaches combine both perspectives by linking aggregate diffusion trajectories with micro-level adoption probabilities [25].

This paper applies a hybrid approach by combining a Bass diffusion model with a logistic regression adoption model. The Bass model determines the aggregate temporal diffusion pathway, while the logistic regression model distributes adoption probabilities across households based on sociodemographic and residential determinants. In contrast to previous work, the household characteristics used for adoption modeling are derived from a spatially localized synthetic population rather than directly from survey observations. This design reflects the fact that the synthetic population provides detailed household characteristics but does not include all behavioral and attitudinal drivers of EV adoption, such as environmental concern or innovation affinity. The model therefore does not aim to explain aggregate EV diffusion entirely from the bottom up, but to allocate a given national diffusion pathway to households and GPS-exact residential locations. Additional adoption drivers could be integrated if they can be linked to synthetic households through sociodemographic proxies, spatial indicators, or additional data sources.

Overall, integrating synthetic population generation, optimization-based household-to-building assignment, and hybrid EV diffusion modeling provides a unified framework that links aggregate EV diffusion to household-level adoption at GPS-exact residential locations. This enables a differentiated temporal, spatial, and sociodemographic analysis of EV diffusion at distribution-grid-relevant scales.

3. Methodology

In the following, we describe the three methodological steps in detail, namely synthetic population generation, household-to-building matching, and adoption modeling. Figure 2 provides an overview of the methodological pipeline and the required input data.

3.1. Microsimulation of the synthetic population

Microdata are large, representative surveys that contain information on individuals and households, including income, age, gender, household size, and education [61–63]. Due to privacy constraints, microdata are typically only available for large spatial units (e.g., national or federal-state level). As a result, analyses at very high spatial resolution are not directly possible without microsimulation. To identify which households from the microdata are most relevant for a given region, aggregated marginal distributions at higher spatial resolution are required. Such marginals for selected attributes, for example, household size, employment status, or education, are available at different spatial levels, for instance, at the municipal level or at the grid level [64].

We simulate the synthetic population using IPU [45] and extend it to a two-level procedure that calibrates household weights simultaneously to marginal distributions available at both a macro level and a grid level. Let N denote the number of households in the microdata sample and G the number of spatial grids. For each IPU iteration t, a weight $w_{ig}^{(t)}$ is

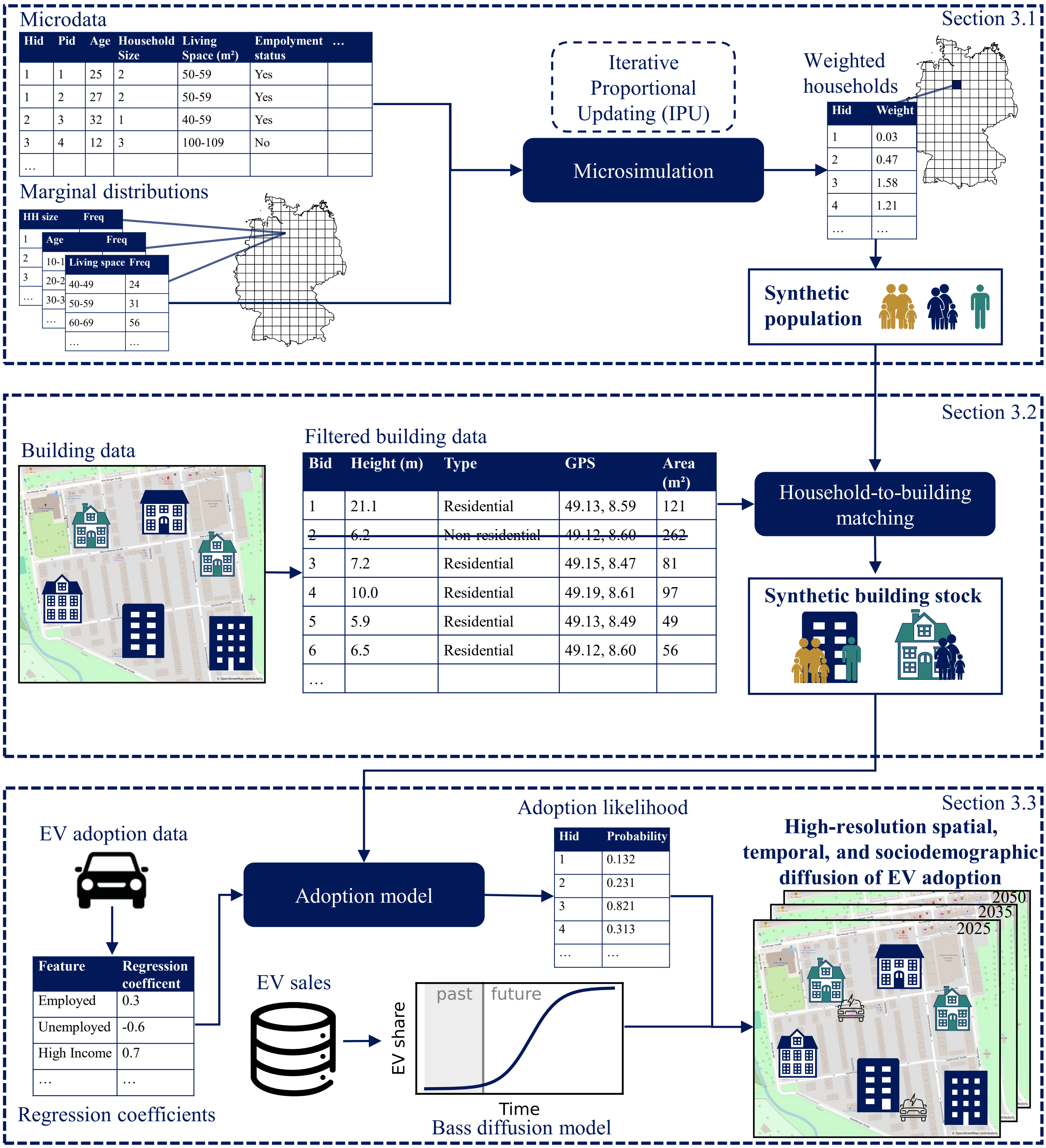

Fig. 2: Schematic overview of the methodological pipeline of this paper. In the first step, a synthetic population is generated for each grid cell using microsimulation (IPU) based on microdata and high-resolution marginal distributions. In the second step, synthetic households are optimally assigned to georeferenced buildings to obtain GPS-exact residential locations. In the third step, a logistic regression model is calibrated on adoption data to estimate household-specific adoption probabilities from sociodemographic determinants. Macroscopic diffusion is represented by a Bass diffusion model, and the annual rollout is stochastically allocated to households according to their estimated adoption probabilities.

assigned to each household i in grid g. Initially, all weights are set to one, i.e., $w_{ig}^{(0)} = 1$.

Macro-level calibration. For each control variable $j = 1, \dots, J$, the current weighted total across all grids is computed as

$$S_j^{(t,\text{macro})} = \sum_{g=1}^{G} \sum_{i=1}^{N} a_{ij}\, w_{ig}^{(t)}, \qquad \forall j \tag{1}$$

where a_{ij} denotes the value of attribute j for household i. Let c_j^{macro} denote the corresponding macro-level marginal total. Weights are then adjusted proportionally across all grids according to

$$w_{ig}^{(t+1/2)} = w_{ig}^{(t)} \cdot \frac{c_j^{\text{macro}}}{S_j^{(t,\text{macro})}}, \qquad \forall i, g \text{ with } a_{ij} > 0, \forall j. \quad (2)$$

Grid-level calibration. Subsequently, for each grid g and control variable j, the weighted total is computed within the grid:

$$S_{jg}^{(t+1/2,\,\text{grid})} = \sum_{i=1}^{N} a_{ij}\, w_{ig}^{(t+1/2)}, \qquad \forall j, g. \quad (3)$$

Let c_{jg}^{grid} denote the corresponding grid-level marginal total. Weights are then updated within each grid as

$$w_{ig}^{(t+1)} = w_{ig}^{(t+1/2)} \cdot \frac{c_{jg}^{\text{grid}}}{S_{jg}^{(t+1/2,\,\text{grid})}}, \qquad \forall i \text{ with } a_{ij} > 0, \forall j, g. \quad (4)$$

An iteration t consists of sequential macro-level and grid-level adjustments over all control variables.

Convergence criterion. After each iteration, the average relative deviation across all macro- and grid-level constraints is computed as

$$\delta^{(t)} = \frac{1}{K}\left[\sum_{j\in\mathcal{J}^{\text{macro}}} \rho_j^{(t,\text{macro})} + \sum_{g=1}^{G}\sum_{j\in\mathcal{J}_g^{\text{grid}}} \rho_{jg}^{(t,\text{grid})}\right], \quad (5)$$

with

$$\rho_j^{(t,\text{macro})} = \left|\frac{S_j^{(t,\text{macro})} - c_j^{\text{macro}}}{c_j^{\text{macro}}}\right|,$$

$$\rho_{jg}^{(t,\text{grid})} = \left|\frac{S_{jg}^{(t,\text{grid})} - c_{jg}^{\text{grid}}}{c_{jg}^{\text{grid}}}\right|,$$

$$\mathcal{J}^{\text{macro}} = \left\{ j \in \{1,\dots,J\} : c_j^{\text{macro}} > 0 \right\},$$

$$\mathcal{J}_g^{\text{grid}} = \left\{ j \in \{1,\dots,J\} : c_{jg}^{\text{grid}} > 0 \right\},$$

$$K = \left|\mathcal{J}^{\text{macro}}\right| + \sum_{g=1}^{G}\left|\mathcal{J}_g^{\text{grid}}\right|,$$

where K denotes the number of active constraints, and $\mathcal{J}^{\text{macro}}$ and $\mathcal{J}_g^{\text{grid}}$ denote the sets of control variables with strictly positive targets at the macro and grid level, respectively.

The algorithm terminates when the improvement Δ falls below a predefined threshold ε

$$\Delta = \left|\delta^{(t-1)} - \delta^{(t)}\right| < \varepsilon. \quad (6)$$

Household sampling. After convergence of the two-level IPU, a calibrated weight w_{ig} is available for each household i and grid cell g. The resulting weights do not directly define a synthetic population, because they are generally non-integer and cannot be represented as discrete household records. An additional sampling step is therefore required to convert the fractional weights into an integer set of households for each grid cell. In the spatial microsimulation literature, a common procedure for this transformation is the Truncate–Replicate–Sample (TRS) method [43, 65, 66]. TRS first extracts the integer part of each calibrated weight (truncate) and deterministically replicates households accordingly (replicate). The remaining fractional parts are then interpreted as sampling probabilities to stochastically allocate the residual households (sample) [66]. Because in our high-resolution setting, grid-level populations are small compared to the microdata sample, the weights w_{ig} are typically less than 1. Therefore, TRS provides no advantage over direct Monte Carlo sampling.

For this reason, we draw the observed number of households N_g in each grid cell g with replacement according to the probability p_{ig}, which is calculated by:

$$p_{ig} = \frac{w_{ig}}{W_g}, \qquad \text{with } W_g = \sum_{i=1}^{N} w_{ig}, \qquad \sum_{i=1}^{N} p_{ig} = 1. \quad (7)$$

This yields an initial Monte Carlo realization. To further improve the reconstruction of grid-level characteristics, we apply a random search step: (i) we remove one randomly selected household, (ii) propose a set of candidate replacements sampled from the same probability distribution, and (iii) accept the replacement that yields the largest reduction in the total grid-level reconstruction error. Optionally, the objective function can include a normalized excess-demand term that penalizes cases in which the aggregate living area demand of the sampled households exceeds the available residential living area in the building data for grid cell g. The procedure terminates after a fixed number of attempts or once no further improvement is observed for a predefined number of consecutive steps.

3.2. Household-to-building matching

In the second step, synthetic households are assigned to georeferenced residential buildings. The matching is performed separately within each grid cell, so that every matched household is associated with a specific building. This building-level localization is required for the subsequent high-resolution spatial diffusion simulations.

The allocation of households to buildings belongs to the class of Generalized Assignment Problems (GAP). Households correspond to items with resource demands (e.g., required living area), whereas buildings represent capacity-constrained agents providing limited living space. Assigning a household to a building consumes capacity and incurs a cost defined by an attribute-based mismatch function. The formulation extends the classical GAP in two directions. First, households may remain unassigned at a penalty cost, which corresponds to a GAP with rejection. Second, unused building capacity is explicitly penalized in the objective, which yields a soft-capacity extension that promotes efficient space utilization. The resulting optimization problem is NP-hard and is solved as a binary integer linear program (BILP).

Let H denote the set of households i and B the set of buildings j. Each household i requires living area $A_i \geq 0$, and each building j provides living area capacity $C_j \geq 0$. In addition, each household carries an attribute a_i (e.g., the residential building type associated with the household), and each building is characterized by the corresponding observed attribute b_j.

The binary decision variable $x_{ij} \in \{0,1\}$ indicates whether household i is assigned to building j, and $u_i \in \{0,1\}$ indicates whether household i remains unassigned. To explicitly represent unused living area, we introduce a nonnegative slack variable $s_j \geq 0$ for each building.

Mismatch between household attribute a_i and building attribute b_j is penalized via an arbitrary, user-defined nonnegative function $g(a_i, b_j) \geq 0$, which is treated as a parameter. The objective minimizes (i) unused area, (ii) unassigned households, and (iii) attribute mismatch penalties:

$$\min \quad \omega \sum_{j \in B} s_j + \lambda \sum_{i \in H} \sum_{j \in B} g(a_i, b_j)\, x_{ij} + \beta \sum_{i \in H} u_i, \tag{8}$$

where $\omega, \lambda, \beta \geq 0$ are the penalties for unused living area, attribute mismatches, and unassigned households, respectively.

Each household must be assigned to exactly one building or remain unassigned:

$$\sum_{j \in B} x_{ij} + u_i = 1 \quad \forall i \in H. \tag{9}$$

Building capacities are enforced through the living-area balance with slack:

$$\sum_{i \in H} A_i x_{ij} + s_j = C_j \quad \forall j \in B. \tag{10}$$

This approach yields an optimal matching of households to buildings based on living area and additional attributes, which is then used to stochastically allocate EV adoption according to household-level adoption likelihoods.

3.3. EV adoption

In the third step, EV adoption is modeled using a hybrid approach that combines a macroscopic diffusion perspective with a microscopic household-level adoption model. At the macroscopic level, the temporal rollout of EVs is represented by a Bass diffusion model, which determines the cumulative EV stock over time. At the microscopic level, an empirically calibrated logistic regression model estimates household-specific adoption likelihoods based on sociodemographic and residential characteristics, which are then used to allocate the macroscopic EV rollout to individual synthetic households.

The temporal diffusion of EVs is described by the Bass model [67]:

$$N(t) = M \frac{1 - e^{-(p+q)t}}{1 + \left(\frac{q}{p}\right) e^{-(p+q)t}}, \tag{11}$$

where $N(t)$ denotes the cumulative EV stock at time t, M the market potential, p the coefficient of innovation, and q the coefficient of imitation.

The macroscopic EV rollout is then allocated to households based on their estimated propensity to adopt an EV. Previous literature has identified several sociodemographic determinants of EV adoption, including education [54–56], income [55, 56], age [54, 57–59], gender [54], and household size [54, 58], among others [60]. Building on these findings, the adoption likelihood of each synthetic household is estimated using a weighted logistic regression model calibrated on observed adoption data. For household i, the probability of EV adoption is given by

$$\pi_i = \Pr(Y_i = 1 \mid \mathbf{x}_i) = \frac{1}{1 + \exp\left[-\left(\beta_0 + \mathbf{x}_i^\top \boldsymbol{\beta}\right)\right]}, \tag{12}$$

where Y_i is a binary indicator of EV adoption, $\mathbf{x}_i$ is the vector of sociodemographic characteristics, β_0 is the intercept, and $\boldsymbol{\beta}$ is the vector of regression coefficients.

To determine the number of vehicles available for potential electrification at the household level, a car ownership model is additionally applied. Specifically, a multinomial logistic regression model, which is commonly used in vehicle ownership analysis [68], is estimated on vehicle ownership data to predict the probabilities that a household owns zero, one, two, or at least three cars. These categories follow the ownership classes reported in the empirical mobility data used for the case study.

Let p_{ik} denote the predicted probability that household i owns k vehicles for $k \in \{0, 1, 2, 3+\}$. The conditional probabilities used for the sequential assignment of the first three vehicles are given by

$$q_{i1} = 1 - p_{i0}, \tag{13}$$

$$q_{i2} = \frac{p_{i2} + p_{i,3+}}{p_{i1} + p_{i2} + p_{i,3+}}, \tag{14}$$

$$q_{i3} = \frac{p_{i,3+}}{p_{i2} + p_{i,3+}}. \tag{15}$$

Since the multinomial model does not distinguish between exactly three and more than three vehicles, additional vehicles beyond the third are assigned using a constant continuation probability

$$q_{ik} = \delta, \qquad k \geq 4, \tag{16}$$

where $\delta \in (0, 1)$ implies a geometrically decaying tail for households with more than three vehicles.

These conditional probabilities are used to assign vehicles sequentially to households until the total market potential M is reached. The resulting synthetic vehicle stock forms the basis of the subsequent EV diffusion process. At the initial time step t_0, the car ownership model assigns each household a total number of vehicles available for electrification. The EV diffusion model then determines which of these vehicles are electric over time according to the estimated household adoption likelihoods and the macroscopic Bass diffusion trajectory.

This yields a high-resolution representation of EV adoption with yearly temporal, GPS-exact spatial, and household- and person-level sociodemographic detail. More generally, the proposed framework is transferable to other technologies, such as photovoltaic systems and heat pumps.

4. Input data

This section describes the input data used for the case study of EV diffusion in Germany. The main input parameters are summarized in Appendix Table 5.

4.1. Microdata and marginals

The synthetic population is based on the 2022 German Microcensus [61] and the 2022 German Census [64]. The Microcensus is representative for Germany, comprises approximately 680,000 persons, and provides household- and person-level microdata for constructing the synthetic population. Specifically, we consider three groups of variables: person-level attributes, including age, gender, education, and employment status; household-level attributes, including household size, household type, and net household income; and building-related attributes, including residential building type, building age, and living area (see Table 2). The selected attributes are required to estimate household-level EV adoption likelihoods. In addition, the building-related variables are used in the subsequent assignment of households to buildings. To preserve regional representativeness, the Microcensus is filtered by federal state so that each municipality draws its donor households from the corresponding state-level sample.

The marginal distributions required for the microsimulation are obtained from the 2022 German Census [64]. Marginals are used at two spatial levels, namely the municipal level and the 100×100 m grid-cell level. At the municipal level, the Census provides information on education, gender, and employment status. At the 100 × 100 m grid-cell level, it provides household size, household type, living area, and age as household- or person-related control totals. The municipal and grid-cell marginals are used as control totals in the two-level iterative proportional updating (IPU) procedure to weight households within each grid cell of a municipality (see Table 2). Owing to confidentiality restrictions, some grid cells do not contain the full set of attributes or include modified values. Net household income is not available at either the municipal or the grid-cell level and is therefore weighted indirectly through the remaining control variables. The same applies to building type and building age, which are available at the grid-cell level only as building counts rather than household counts and therefore can not be used as direct IPU constraints.

To spatially link municipalities to grid cells and obtain the geographic location of each municipality, we use the 100 × 100 m grid data provided by the German Federal Agency for Cartography and Geodesy [69]. The data are available in INSPIRE [70] format and assign each grid cell to its area-dominant municipality as of 2019.

4.2. Building data

To represent the residential building stock, we combine two global building datasets: the Global Human Settlement Open Building Attribute Table (GHS-OBAT) [71] and the Global Building Atlas (GBA) [72]. GHS-OBAT contains information on approximately 2.3 billion buildings worldwide, including use type, construction period, footprint area, height, and location. The GBA covers more than 2.75 billion buildings globally and provides building polygons and height information. In the GBA, building heights are derived at a spatial resolution of 3 × 3 m [72].

Both datasets were selected because they are globally available and can therefore be adapted to regional contexts beyond the German case study. For the present analysis, both datasets are filtered to Germany. Residential buildings are first identified using GHS-OBAT, and the resulting residential building set is spatially linked with the GBA to add building height information. Heights are primarily taken from the GBA and supplemented with GHS-OBAT values where GBA height information is missing. Building height is required to estimate the number of stories and, in turn, the total living area of each building.

To estimate the number of stories, we assume an average story height of 3.0 m, consistent with typical German residential building geometries and standard construction practice as represented in the IWU building typology [73]. Combined with the building footprint area, this yields an estimate of the total living area for each building. Together with building age and the inferred building type, this information is used in the subsequent household-to-building matching (Table 2).

For building type, GHS-OBAT only identifies residential buildings and does not distinguish single-family from multi-family houses. The building type used in the matching is therefore inferred from the assignment itself: buildings occupied by exactly one household are treated as single-household buildings, whereas buildings occupied by two or more households are treated as multi-family buildings. A penalty is added if this occupancy-based building type is inconsistent with the expected residential building type of the assigned household.

For building age, households and buildings are represented by age classes that are translated into year intervals. If the household-side and building-side intervals overlap, no penalty is applied. Otherwise, the penalty increases linearly with the temporal distance between the two intervals. Missing information for building type or building age does not generate a penalty. Additional details are provided in Appendix A.

4.3. Adoption data

The Bass diffusion model is calibrated using empirical stock data on battery electric vehicles (BEVs) in Germany for the period 2014–2025, obtained from the German Federal Motor Transport Authority [74].

The household-level EV adoption model is estimated using data from Mobility in Germany 2023 (MiD 2023) [75]. Overall, the MiD comprises approximately 420,000 individuals and reflects a weighted EV share of around 7%. This is higher than the current German passenger-car stock, in which battery-electric vehicles account for 4.1% of registered cars as of 1 January 2026 [76]. Since EV adoption is modeled at the household level, individual-level characteristics are aggregated to the household level and used to estimate household-specific adoption likelihoods. The model includes the following sociodemographic and residential determinants, selected to be consistent with the attributes available in the synthetic population: education, age, building type (single-family or multi-family house), household size, household income, and federal state (Table 2).

MiD also provides information on household car ownership in the categories zero, one, two, and at least three cars. These data are used to calibrate the multinomial car ownership model. Based on the predicted category probabilities, household-specific conditional probabilities are then derived for the sequential assignment of vehicles. For households with more than three vehicles, additional vehicles are represented by assuming a constant conditional continuation probability of $\delta = 0.25$, chosen as a conservative assumption informed by the high vehicle-count categories in the 2022 US National Household Travel Survey [77].

Table 2
Attributes included in the synthetic population and their use as IPU control marginals, building-matching variables, and EV adoption determinants.

Attributes	Marginals	Matching	Adoption
Age	Grid cell		✓
Gender	Municipality		
Education	Municipality		✓
Employment	Municipality		
Household size	Grid cell		✓
Household type	Grid cell		
Household income			✓
Living area	Grid cell	✓	
Building type		✓	✓
Building age		✓	

The Census marginal column indicates whether the attribute is available as a Census control total at the municipal level or at the 100×100 m grid-cell level. Gender and employment status are available in Mobility in Germany 2023, but are not included in the EV adoption model due to collinearity with other variables. Federal state is additionally included as a regional parameter in the EV adoption model.

5. Results

The synthetic population reproduces the empirical population characteristics with reasonable accuracy, given the partial inconsistency of the available Census controls. Across municipalities, the average relative deviation from the Census marginals decreases from 27% after Iterative Proportional Updating (IPU) to 15% after household sampling (Fig. 3a). This metric should be interpreted as a conservative discrepancy measure, because it averages relative deviations across marginal categories whose target totals are not always mutually consistent. In particular, the aggregated comparison in the Appendix (Fig. 7) shows that the published household-level marginals do not sum to the same total as the overall household-count target. Since the synthetic population assigns household size, household type, and living-area information to all households, while the corresponding Census marginals cover fewer households, matching the total household count necessarily produces positive deviations for these household-level attributes, especially for living area. The detailed national-level comparison in the Appendix (Fig. 6) nevertheless shows that the drawn households largely preserve the empirical distributional patterns across categories. Sampling reduces the municipal-level deviation because households are drawn independently for each grid cell, allowing the required number of households to be matched locally and limiting the accumulation of small deviations across the larger number of grid cells relative to municipalities. The final sample further incorporates the optional living-area demand penalty, which discourages samples whose aggregate living-area demand exceeds the available residential living area in the building data. Compared with sampling without this penalty, the resulting living-area distribution is shifted toward smaller dwellings, reducing the overrepresentation of large flats and improving compatibility with the subsequent household-to-building matching. Based on the 2019 municipal structure, the analysis covers 11,007 municipalities across Germany; for 231 municipalities, no synthetic population could be generated because the corresponding areas are either uninhabited or lack the required Census information. Overall, the remaining deviations mainly reflect inconsistencies and incomplete coverage in the available Census controls rather than a failure of the synthetic reconstruction, while the main empirical distributional patterns are retained.

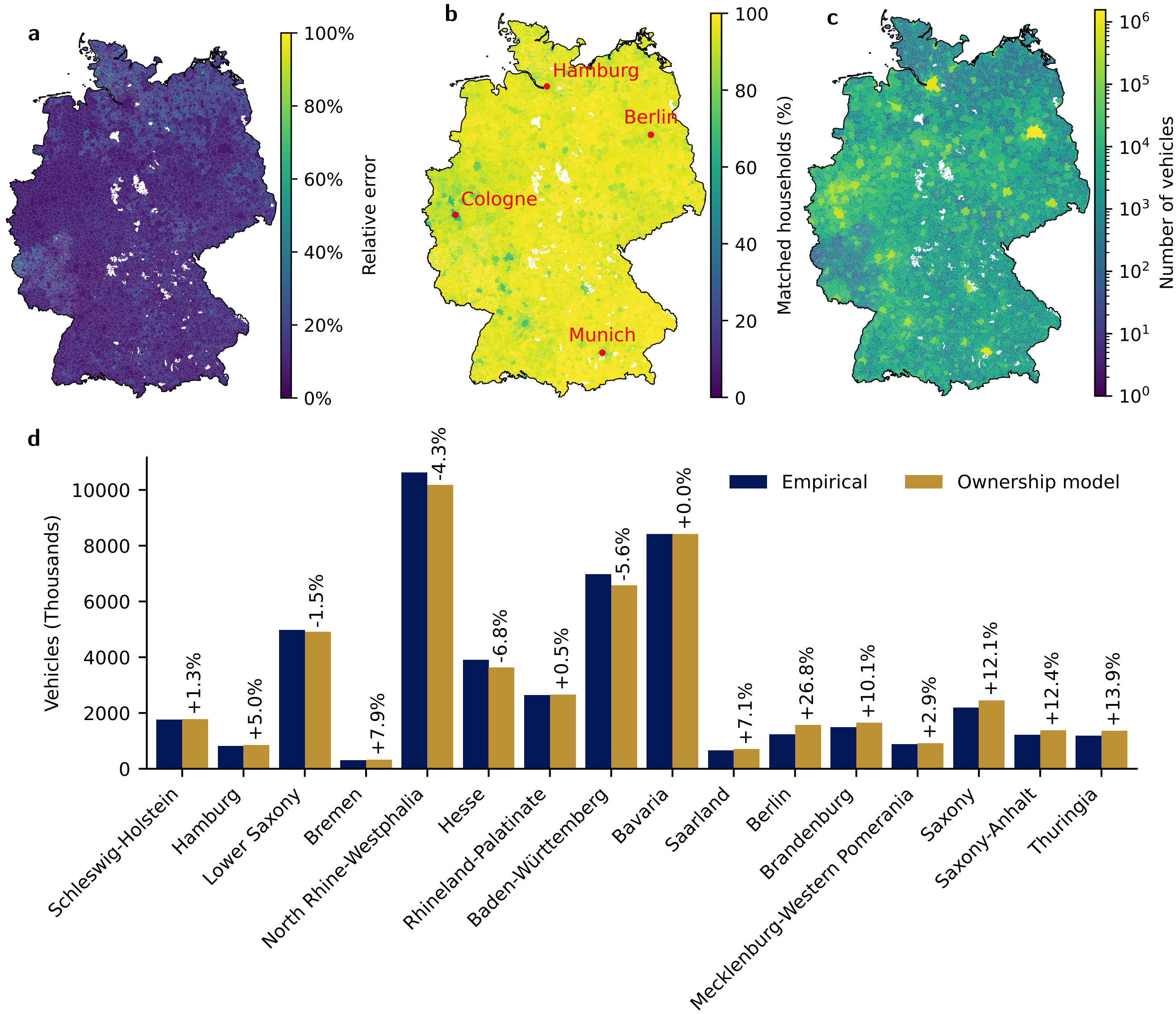

Fig. 3: Validation of the synthetic population, household-to-building matching, and car ownership model. The synthetic population is evaluated against Census marginals using the average relative error after sampling for each municipality in Germany (**a**), calculated according to Eq. 5. The household-to-building matching is assessed by the share of households successfully matched to residential buildings by municipality (**b**). The spatial distribution of vehicles assigned by the car ownership model is shown at the municipal level (**c**). The car ownership model is validated at the federal state level by comparing modeled vehicle counts with registered passenger cars in 2025 reported by the German Federal Motor Transport Authority [78] (**d**). White municipalities indicate areas without a synthetic population, either because they are uninhabited, such as nature reserves, or because required Census information is missing.

Households can be spatially assigned to residential buildings with high coverage across Germany. The household-to-building matching reaches a mean matching rate of 91% across grid cells (Fig. 3b), compared with 83.7% without the living-area demand penalty. This corresponds to approximately 36 million of 39.5 million households and about 77 million individuals matched to buildings. To avoid excessive computation time in individual grid cells, the optimization was solved with a 5% optimality gap and a time limit of 20 s per grid cell, after which the best available solution was retained. Under these settings, the solver reached optimality for 97% of grid cells. The remaining grid cells were either not solved to optimality within the time limit or could not be solved because no building information was available. The assignment retains key building characteristics, although mismatches remain: about 11% of matched households differ from their expected building type and 28% from their expected building age. These mismatches indicate that the matching prioritizes household coverage and living-area feasibility over perfect agreement in all building attributes.

Table 3
EV adoption model: training and evaluation summary.

Measure	Value
Sample composition	
Households after vehicle-ownership filter	189,562
Households dropped due to missing building type	7,234
Households dropped due to missing EV ownership status	451
Households used for model estimation	181,877
Households with EV	19,217
Households without EV	162,660
EV share in model sample, unweighted	10.6%
EV share in model sample, weighted	7.7%
Training fit (80% split)	
McFadden pseudo-R^2	0.102
Adjusted McFadden pseudo-R^2	0.101
McKelvey–Zavoina pseudo-R^2	0.240
Test-set predictive performance (20% split)	
AUC-ROC	0.741
Log loss	0.242
Accuracy	0.891
Precision	0.215
Recall	0.167
F1-score	0.188

For the EV diffusion analysis, the building-type mismatch is particularly relevant because single-family houses enter the adoption model.

The car ownership model provides the vehicle stock used as the basis for subsequent electrification. The model training and evaluation summary is reported in Table 6, and the direction and significance of the determinants are summarized in Table 7. The resulting municipal distribution of assigned vehicles is shown in Fig. 3c. For validation, the modeled vehicle counts are aggregated to the federal state level and compared with registered passenger cars in 2025 reported by the German Federal Motor Transport Authority [78] (Fig. 3d). In this comparison, the model reproduces registered passenger car counts with a vehicle-weighted average error of 4.9%. The assigned vehicle stock then serves as the basis for subsequent electrification by the household-level adoption model.

The household-level adoption model identifies clear sociodemographic, residential, and regional determinants of electric vehicle adoption, while also reflecting the limited observability of household-level adoption drivers. The logistic regression model reaches an adjusted McFadden pseudo-R^2 of 0.101 (Table 3). Since this metric measures improvement in model likelihood relative to an intercept-only model rather than the share of variance explained, the value indicates a meaningful but incomplete ability to distinguish adopting from non-adopting households. This is consistent with the absence of several potentially relevant behavioral and attitudinal drivers, such as environmental concern, innovation affinity, and charging access. The model nevertheless shows clear and statistically significant associations: household net income and residence in single-family houses are positively associated with electric vehicle adoption, while age structure and education also influence adoption probabilities (Table 4). Federal state effects remain relevant after accounting for observed household characteristics, indicating that regional differences are not fully captured by the available sociodemographic and residential variables.

The spatially resolved diffusion model shows that national electric vehicle growth translates into markedly different local adoption trajectories. Figure 4 illustrates this heterogeneity for Germany, Berlin, and two selected 500 × 500 m grid cells in Berlin (Fig. 4a–c). At the national level, the temporal development follows the Bass diffusion trajectory fitted to historical vehicle-stock data from the German Federal Motor Transport Authority [74] (Fig. 4d). The adoption trajectories for Berlin and the selected grid cells demonstrate how this national diffusion pathway differs across spatial scales (Fig. 4e–f). In the selected example, grid cell A at the urban fringe shows a faster increase in electric vehicle share than the city center grid cell B, particularly between 2030 and 2040. This difference is consistent with the sociodemographic and residential structure of the two grid cells: grid cell A has a higher average net household income and, in particular, a substantially higher share of single-family houses than grid cell B (Appendix Fig. 8).

Beyond the selected Berlin examples, the model reveals strong East–West differences in electric vehicle diffusion across Germany. The spatial distribution of the electric vehicle share in 2035 shows higher diffusion levels in West

Table 4
Determinants of EV adoption based on the logistic regression EV adoption model.

Feature	Coefficient	Odds ratio	Standard error
Constant	-5.895^{***}	0.003	0.083
Household net income	0.541^{***}	1.717	0.012
Building type: single-family house	0.453^{***}	1.573	0.027
Household size	0.086^{***}	1.090	0.012
Age: 0–9 years	-0.201^{***}	0.818	0.047
Age: 10–19 years	-0.273^{***}	0.761	0.042
Age: 20–29 years	-0.347^{***}	0.707	0.032
Age: 30–39 years	-0.236^{***}	0.790	0.023
Age: 50–59 years	-0.044	0.957	0.022
Age: 60–69 years	-0.092^{***}	0.912	0.025
Age: 70–79 years	-0.230^{***}	0.795	0.032
Age: 80+ years	-0.609^{***}	0.544	0.051
Education: no degree	0.102^{**}	1.107	0.038
Education: lower level	0.090^{**}	1.094	0.028
Education: upper level	0.335^{***}	1.398	0.027
State: Baden-Württemberg	0.288^{***}	1.334	0.064
State: Bavaria	0.289^{***}	1.335	0.063
State: Berlin	-0.206^{*}	0.813	0.102
State: Brandenburg	-0.105	0.900	0.091
State: Bremen	-0.191	0.826	0.169
State: Hamburg	-0.123	0.884	0.108
State: Hesse	0.146^{*}	1.157	0.069
State: Lower Saxony	0.178^{**}	1.195	0.067
State: Mecklenburg-Western Pomerania	-0.363^{**}	0.695	0.117
State: North Rhine-Westphalia	0.224^{***}	1.251	0.062
State: Rhineland-Palatinate	0.208^{**}	1.232	0.074
State: Saarland	0.182	1.199	0.109
State: Saxony	-0.230^{*}	0.794	0.090
State: Saxony-Anhalt	-0.063	0.939	0.102
State: Thuringia	-0.262^{*}	0.769	0.104

Age and education variables are measured at the household level and indicate the number of household members in the respective age or education category. The reference category for age is 40–49 years; the reference category for state is Schleswig-Holstein. Significance levels: $^{***}p < 0.001$, $^{**}p < 0.01$, $^{*}p < 0.05$.

Germany than in East Germany (Fig. 5a). This difference persists over time, with East Germany lagging behind West Germany throughout the diffusion pathway (Fig. 5c). The regional contrast is more consistent with variation in income and residential building structure than with age (Appendix Fig. 9). The synthetic population is only slightly older in East Germany than in West Germany, with average ages of 45.0 and 43.5 years, respectively, closely matching the corresponding Census 2022 pattern of about 46 and 44 years [64]. In contrast, differences in household net income and single-family house share are more pronounced. Average net household income is approximately 12% higher in West Germany than in East Germany, which is close to the corresponding Microcensus difference of about 14% [61]. The single-family house share is about 36% higher in West Germany than in East Germany, exceeding the corresponding Census difference of about 14% [64]. This stronger difference should be interpreted in light of the fact that building type is not available as a direct IPU control marginal. Because both income and single-family house residence increase adoption probabilities in the household-level adoption model, these determinants likely contribute substantially to the lower diffusion levels observed in East Germany.

A further spatial contrast emerges between urban and rural municipalities, with rural municipalities slightly ahead in electric vehicle adoption. Figure 5b shows the electric vehicle share in 2035, with urban municipalities indicated by dots. The highlighted examples of Berlin, Bremen, Frankfurt, Munich, and their surrounding municipalities illustrate that adoption levels differ considerably across urban regions. When all urban and all rural municipalities are aggregated into two temporal pathways, rural municipalities maintain slightly higher electric vehicle shares throughout most of

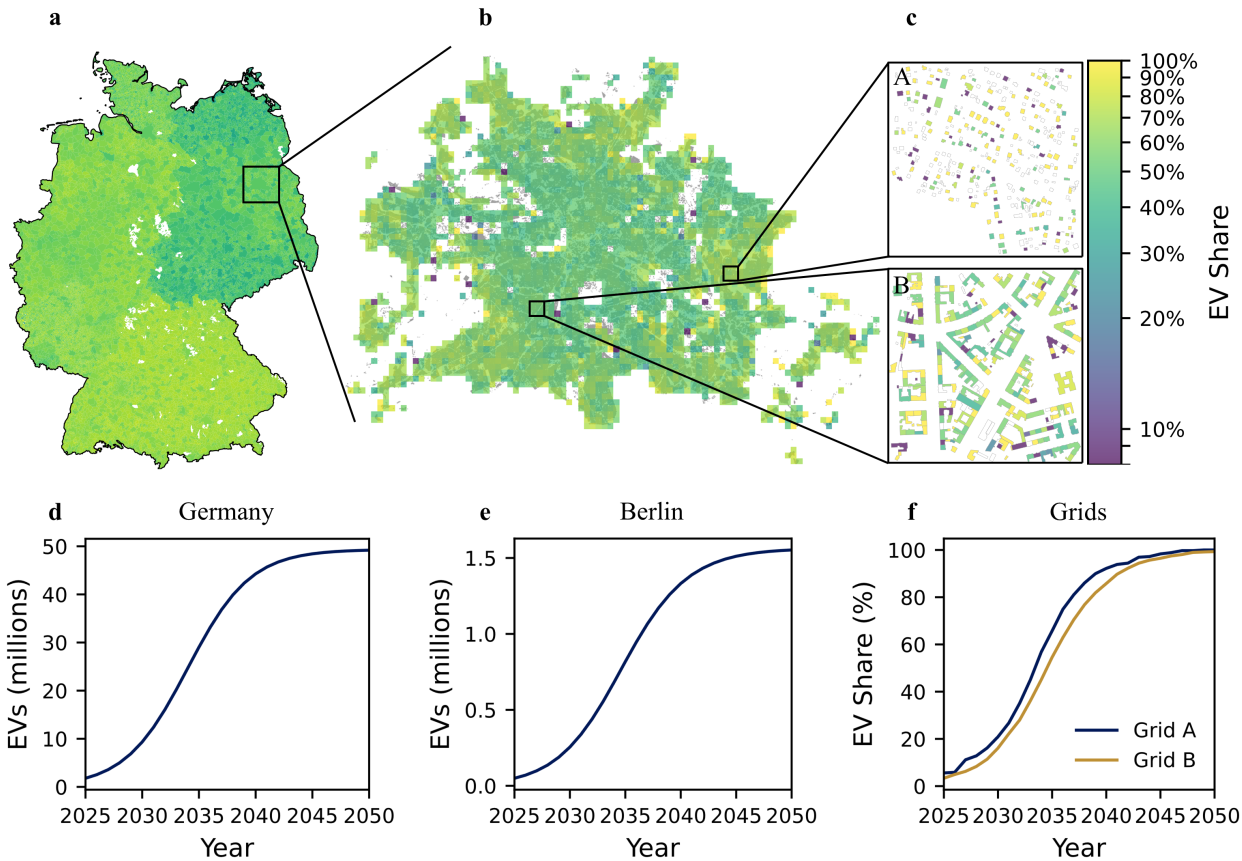

Fig. 4: Spatial and temporal distribution of electric vehicles across different spatial scales. The spatial distribution of the electric vehicle share in 2035 is shown at the municipal level for Germany (**a**), at the 500×500 m grid-cell level for Berlin (**b**), and at the building level for two selected example grid cells in Berlin (**c**). The temporal development of electric vehicle diffusion from 2025 to 2050 is shown for Germany, Berlin, and the selected grid cells, respectively (**d**–**f**). White buildings in the grid-cell examples indicate either buildings occupied by households without vehicles or buildings without matched households.

the diffusion pathway (Fig. 5d). This aggregate pattern is consistent with the higher share of single-family houses in rural municipalities, which increases adoption probabilities in the household-level adoption model (Appendix Fig. 10).

6. Discussion

This study addresses a central gap in spatial EV diffusion modeling by linking household-level adoption behavior with GPS-exact residential locations. The results show that national EV growth can be translated into highly localized adoption trajectories when synthetic population modeling, household-to-building matching, car ownership modeling, and household-level adoption probabilities are combined in one framework. This combined approach makes it possible to move beyond aggregate EV stock projections by estimating not only how many vehicles are likely to be electrified, but also where these vehicles are located. The validation results show that the synthetic population, building assignment, and car ownership model reproduce the key population, residential, and vehicle-stock patterns required for allocating EV adoption spatially across municipalities, grid cells, and buildings. At the same time, the diffusion results demonstrate why this level of spatial detail matters: EV adoption differs substantially between regions, municipalities, and grid cells, as well as within individual grid cells. These differences are strongly shaped by sociodemographic and residential characteristics, particularly household income and single-family houses. The framework therefore contributes to the literature by explicitly connecting household characteristics, residential location, and technology adoption at GPS-exact spatial resolution in a single modeling framework.

The EV adoption model shows comparatively strong explanatory power for a household-level model based primarily on sociodemographic and residential characteristics. Studies with a comparable information set report McFadden pseudo-R^2 values of about 0.04–0.07 [27, 80–83], whereas models that additionally include detailed vehicle attributes, policy variables, mobility indicators, or latent attitudinal factors report higher values, ranging approximately from 0.15 to 0.50 [84–87]. The adjusted McFadden pseudo-R^2 of 0.101 obtained here is therefore toward the upper end of models relying mainly on sociodemographic and residential characteristics, which may partly reflect the large MiD sample, while remaining below models with richer

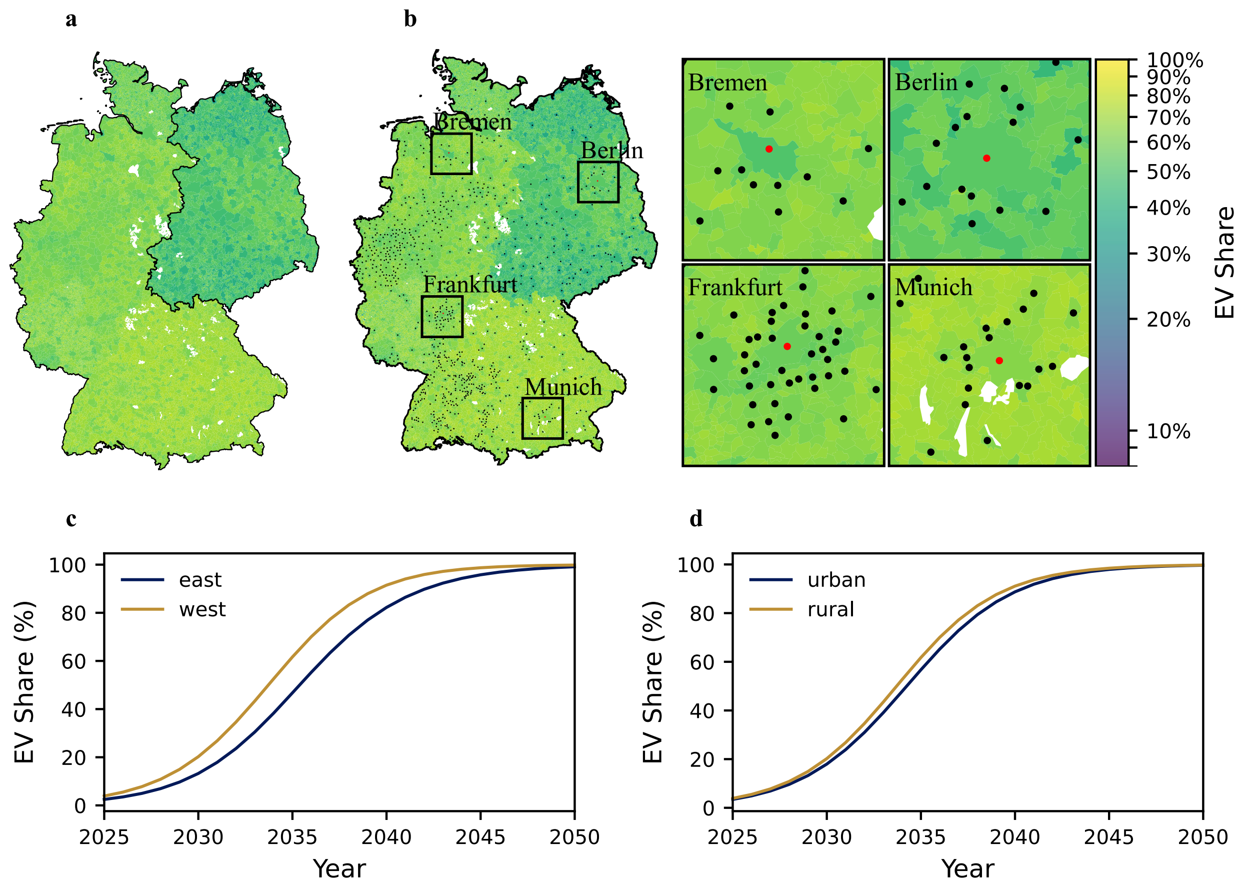

Fig. 5: Spatial and temporal heterogeneity of electric vehicle diffusion in Germany. The electric vehicle share is shown for each municipality in 2035, distinguishing East and West Germany by the indicated East–West boundary (**a**). Urban and rural differences are shown for the same year, with urban municipalities marked by dots (**b**). Panel (**b**) additionally highlights selected urban examples, including Berlin, Bremen, Frankfurt, Munich, and their surrounding municipalities. The temporal development of the electric vehicle share from 2025 to 2050 is shown for East and West Germany as a whole (**c**) and aggregated across all urban and all rural municipalities (**d**). Municipalities are defined as urban if classified as large cities or medium-sized towns, based on the classification of the Federal Institute for Research on Building, Urban Affairs, and Spatial Development [79].

behavioral or choice-experiment information. This supports the hybrid modeling approach, in which the Bass model defines the aggregate diffusion pathway and the adoption model allocates this pathway across households and residential locations based on observed sociodemographic and residential characteristics.

The spatial patterns identified in this study are consistent with the broader literature on EV adoption, but add a more spatially explicit interpretation of these mechanisms. Household income emerges as one of the strongest determinants of adoption, in line with previous studies [57–59, 88]. Residence in a single-family house is another important determinant in our adoption model. Previous studies emphasize related factors such as home ownership [57, 59] and charging access [59]. Single-family houses are likely to capture part of these mechanisms because they more often provide private parking and easier access to home charging. Other significant determinants in our model, including education, age, and household size, are also consistent with earlier findings [54, 57–59]. These determinants help explain the local heterogeneity observed within Berlin: the selected grid cell with higher income and a substantially higher share of single-family houses shows faster EV diffusion than the city center grid cell. This interpretation refers to the selected grid-cell comparison and should not be generalized to all urban-fringe areas, because the spatial distribution of building types remains heterogeneous within Berlin.

The East–West difference in EV diffusion is partly consistent with the sociodemographic and residential structure identified in the results. East Germany shows both lower average household income and a lower share of single-family houses than West Germany, two determinants associated with lower adoption probabilities in the household-level model. Similar regional disparities in EV uptake have also been reported by Speth et al. [89], indicating that the lower diffusion levels observed in eastern Germany are consistent with previous regional analyses. However, the East–West difference should not be interpreted as a purely sociodemographic effect. The federal state information included in the adoption model may also capture unobserved regional characteristics beyond income and residential structure. Previous adoption studies show that EV uptake is associated not only with sociodemographic variables, but also with environmental concern, innovation affinity, and other behavioral or attitudinal factors [54, 55, 60]. However, although such variables can improve the explanatory power of adoption models, they are not available for the synthetic population generated from Microcensus and Census data [61, 64]. The estimated federal state effects should therefore be interpreted as composite spatial effects that may reflect differences in charging infrastructure availability, technology affinity, political preferences, or attitudes toward climate protection, rather than as direct causal effects of administrative location.

The urban–rural contrast further illustrates that settlement structure affects EV adoption, but not in a uniform way. In our results, rural municipalities are slightly ahead of urban municipalities in the aggregate diffusion pathway. This pattern is plausible in the German context because rural municipalities tend to have a higher share of single-family houses. At the same time, the results show substantial heterogeneity across municipalities and urban regions. This mixed pattern is consistent with previous literature, which does not identify a uniform urban effect: while some studies report higher EV adoption in urban areas [58], others find higher adoption probabilities in rural regions or small towns [54]. The urban–rural distinction should therefore be interpreted as an aggregate pattern rather than as a deterministic predictor of local EV adoption.

The results have direct implications for distribution grid and charging infrastructure planning. Since EV adoption is spatially concentrated in households and residential environments with higher adoption probabilities, grid impacts are unlikely to follow the national diffusion pathway uniformly. Instead, local areas with high household income, high share of single-family houses, and favorable regional conditions may experience faster EV uptake and therefore earlier charging-related grid stress. This is particularly relevant for low-voltage grids, where a small number of households with coincident charging demand can already create local constraints. The building-level resolution of the proposed framework can therefore help identify where charging demand is likely to emerge first and where grid reinforcement, public charging infrastructure, or smart charging strategies may become relevant earlier. At the same time, the results show that aggregated spatial units can mask substantial heterogeneity. Municipal or regional EV shares may appear moderate even when individual grid cells or residential clusters already reach much higher adoption levels. High-resolution diffusion modeling therefore provides an important link between national EV scenarios and locally actionable planning information.

The open framework is flexible and transferable to other countries and other household technologies, provided that comparable input data are available. Its core requirements are household microdata, spatially disaggregated census marginals, building data, and technology adoption data. Such data are available in many contexts. National microdata and census sources exist, for example, for the United States [90–92], the United Kingdom [93, 94], Australia [95, 96], France [97, 98], and the European Union [99, 100]. Internationally harmonized sources, such as IPUMS [101, 102], the Luxembourg Income Study, and the Demographic and Health Surveys [103, 104], further support cross-country applications. Ton et al. [43] demonstrate the feasibility of large-scale synthetic population generation by constructing a global synthetic population of approximately seven billion individuals based on Luxembourg Income Study and Demographic and Health Surveys microdata. Building data are increasingly available through global datasets such as GBA and GHS-OBAT [71, 72]. For EV adoption, comparable travel surveys exist for countries such as the United States, the United Kingdom, and France [105–107]. Beyond EVs, the same modeling logic could be applied to other household technologies, such as heat pumps, residential photovoltaics, or air conditioning, if adoption data can be linked to sociodemographic and building characteristics, such as rooftop area or building age. Examples include the German Microcensus and the KfW Energy Transition Barometer for Germany [61, 108], as well as the Residential Energy Consumption Survey for the United States [109]. In addition, recent work on global AC diffusion highlights the importance of linking adoption to income, service access, and energy-poverty concerns [40, 42, 110, 111]. Thus, the proposed framework is not limited to EV diffusion in Germany, but provides a general and adaptable approach for spatially explicit modeling of household technology adoption.

Despite this flexibility, several limitations should be considered when interpreting the spatial diffusion results. First, the framework uses a static representation of the population, building stock, and household-to-building assignment. The synthetic population captures the sociodemographic structure at the baseline year, but it does not dynamically simulate demographic change, such as aging, births, deaths, household formation, separation, or changing household composition. Similarly, the building stock is treated as fixed and therefore does not account for urban development, new residential construction, redevelopment, demolition, or changes in dwelling availability [112]. The household-to-building assignment is also static, meaning that migration, residential relocation, and changing housing choices over time are not represented.

In addition, the household-to-building matching should be interpreted as a lower-bound estimate of building-level household allocation. The model assigns households only where the available building capacity is sufficient under the estimated living-area constraints. As a result, households can remain unmatched in areas where household living-area demand is overestimated, building capacity is underestimated, or building information is incomplete. The improved matching rate of 91% substantially reduces this issue, but the remaining unmatched households imply that building-level household, vehicle, and EV stocks may still be underestimated in areas with uncertain building data. This conservative treatment avoids increasing coverage by assigning households to buildings with uncertain or implausible residential capacity. Future applications could address this limitation by using the height uncertainty reported in GBA to construct sensitivity cases with higher building capacities, or by integrating additional building datasets, such as EUBUCCO [113], to improve building coverage and capacity estimates.

As a result of the static population, building stock, and household assignment, the spatial distribution of adoption determinants remains fixed, while only the electrification of the assigned vehicle stock evolves over time. This design choice reflects the aim of developing a data-driven, low-assumption framework for spatial technology diffusion. More dynamic modeling approaches could relax this assumption. Dynamic microsimulation models can update households over time through aging, births, deaths, household formation, and migration [114–117], thereby allowing adoption determinants to evolve throughout the diffusion period. Similarly, urban microsimulation models can represent where new dwellings are constructed, where existing buildings are redeveloped or demolished, and how the available housing stock changes spatially [118]. Coupling such population and building-stock dynamics with residential location choice models would allow households to move between dwellings over time rather than remain fixed at their initial building assignment [119]. These extensions could improve long-term realism, but would shift the framework from a mainly data-driven spatial allocation model toward a more scenario-dependent representation of population and housing dynamics.

Second, the temporal diffusion pathway is determined by the Bass diffusion model and therefore abstracts from several mechanisms that may influence future EV uptake. These include vehicle price dynamics, policy changes, and charging infrastructure expansion [60]. The EV adoption model is estimated from cross-sectional data and therefore cannot capture dynamic adoption processes, such as the conditional probability of purchasing an additional EV after already owning one. Estimating such transitions would require longitudinal data. Moreover, several potentially important drivers of EV adoption are not observed in the synthetic population, including environmental attitudes, political orientation, technology affinity, and actual charging access. Neighborhood effects have also been identified as relevant for EV adoption [59]. In principle, such effects could be integrated into the proposed spatial framework, but this would require data that link neighborhood-level adoption dynamics to household sociodemographic characteristics. The role of these factors may also change over time, and the determinants of early EV adoption may not fully represent the determinants of mass-market adoption in later diffusion stages. Nevertheless, although the available data do not capture all relevant behavioral and contextual drivers, the EV adoption model shows moderate explanatory power and identifies plausible determinants that are consistent with previous literature.

Future research should build on the spatial detail of the proposed framework by linking the GPS-exact EV diffusion to charging demand and distribution grid models. While this study identifies where and when EV adoption is likely to emerge, the next step is to translate these adoption patterns into temporally resolved charging profiles, including uncontrolled, smart, and potentially bidirectional charging. A promising direction is to generate household-level activity and mobility profiles from sociodemographic characteristics and spatial context, for example using transformer-based deep neural networks trained on time-use and mobility survey data [49, 120]. These activity profiles could determine when vehicles are at home, when trips occur, and when charging demand can arise. In addition, they could be linked to residential electricity demand through a bottom-up household demand model calibrated to empirical data, enabling the assessment of local demand impacts and flexibility potentials. Conceptually, such an approach is similar to Staffell et al. [121], who translate weather-derived heating and cooling indicators into energy demand using calibrated demand coefficients. Combining spatially explicit EV adoption, activity-based mobility profiles, and residential demand modeling would enable assessment not only of where EVs are adopted, but also when and under which charging strategies they may create or relieve local grid constraints. Future work could also improve the adoption layer itself by incorporating more detailed behavioral information, such as environmental attitudes and neighborhood effects, if such data become available at sufficient sociodemographic resolution. Overall, such an extension would provide a stronger basis for locally targeted charging infrastructure planning, distribution grid reinforcement, and flexibility strategies.

7. Conclusion

This study developed a high-resolution technology diffusion model with annual temporal resolution, GPS-exact spatial resolution, and household-level sociodemographic detail for the case of EV diffusion in Germany. By combining a synthetic population, household-to-building matching, car ownership modeling, and EV adoption modeling, the framework translates national EV growth, projected by a Bass diffusion model, into highly localized adoption trajectories. This enables the estimation of not only how many vehicles are likely to be electrified, but also where these vehicles are located.

The results show that the modeling framework provides a robust basis for spatial analysis of EV diffusion. The synthetic population reproduces Census marginals with relatively high accuracy, the household-to-building assignment spatially locates most households in residential buildings, and the car ownership model provides a validated vehicle stock for subsequent electrification. The spatial diffusion results reveal substantial heterogeneity across scales. Within Berlin, selected grid cells show markedly different adoption trajectories, driven by differences in income and residential building structure. At the national level, EV diffusion is higher in West Germany than in East Germany, consistent with regional differences in household income and share of single-family houses. Rural municipalities are slightly ahead of urban municipalities in aggregate, although urban areas themselves show considerable heterogeneity.

These findings highlight the need for highly spatially resolved diffusion frameworks for household technologies, such as heat pumps and residential photovoltaics, because spatial heterogeneity is central to local energy system operation, distribution grid planning, and charging infrastructure planning. Local adoption patterns depend on sociodemographic, residential, and regional characteristics that can be masked by aggregated spatial representations. The proposed framework therefore links household-level adoption decisions with the spatial information needed for local energy system analysis. Future work should connect GPS-exact households and their associated technology stocks, including electric vehicles, with temporally resolved demand profiles to assess when and where local demand peaks may emerge and how they may affect system operation and planning.

Data availability

The input data used in this study are obtained from publicly available or restricted-access data sources. All publicly available input data required to run the workflow are accessible through the links and scripts provided in the GitHub repository associated with this study. The German Microcensus data used for constructing the synthetic population are subject to access restrictions and cannot be redistributed by the authors. To facilitate testing and adaptation of the framework, the repository provides an alternative workflow based on publicly available microdata from the American Community Survey Public Use Microdata Sample [90]. The EV adoption survey data used to estimate the electric vehicle adoption model are also subject to access restrictions and cannot be shared directly. However, the estimated regression coefficients and model specification are provided in the repository, allowing the adoption model to be applied within the proposed framework.

Code availability

The modeling framework developed in this study is written in Python and is publicly and freely available on GitHub at `https://github.com/GitMoritzraab/PySEDM`. The results presented in this study were generated using PySEDM version v0.1.0. The repository contains the code required to construct the synthetic population, perform household-to-building matching, apply the car ownership and EV adoption models, and generate the spatial diffusion results. The full Germany-wide implementation was run on the bwHPC high-performance computing infrastructure because of the large number of municipalities, grid cells, households, and buildings. However, the workflow is modular, and individual municipalities or smaller study regions can be processed on a local laptop or desktop computer.

CRediT authorship contribution statement

Moritz Raab: Conceptualization, Methodology, Validation, Writing - original draft, Investigation, Visualization. **Max Kleinebrahm:** Conceptualization, Methodology, Writing - review & editing, Supervision. **Jonathan Vogl:** Conceptualization, Writing - review & editing. **Tim Signer:** Conceptualization, Writing - review & editing. **Jannik Braun:** Methodology, Visualization. **Wolf Fichtner:** Supervision, Writing - review & editing, Funding acquisition.

Declaration of Competing Interest

The authors declare that they have no known competing financial interests or personal relationships that could have appeared to influence the work reported in this paper.

Acknowledgements

This paper was created in the "Country 2 City - Bridge" project of the "German Center for Future Mobility", which is funded by the German Federal Ministry of Transport.

The authors acknowledge support by the state of Baden-Württemberg through bwHPC.

Declaration of generative AI and AI-assisted technologies in the writing process

During the preparation of this work the authors used ChatGPT in order to improve the readability and language of the manuscript. After using this tool, the authors reviewed and edited the content as needed and take full responsibility for the content of the publication.

References

[1] International Energy Agency. Global EV Outlook 2025: Trends in electric car markets, 2025. URL `https://www.iea.org/reports/global-ev-outlook-2025/trends-in-electric-car-markets-2`. Accessed: 2026-02-11.

[2] International Energy Agency. Global EV Outlook 2025: Outlook for electric mobility, 2025. URL `https://www.iea.org/reports/global-ev-outlook-2025/outlook-for-electric-mobility`. Accessed: 2026-02-11.

[3] Matteo Muratori. Impact of uncoordinated plug-in electric vehicle charging on residential power demand. *Nature Energy*, 3:193–201, 2018. doi: 10.1038/s41560-017-0074-z.

[4] Mathias Müller, Yannic Blume, and Janis Reinhard. Impact of behind-the-meter optimised bidirectional electric vehicles on the distribution grid load. *Energy*, 255:124537, September 2022. ISSN 03605442. doi: 10.1016/j.energy.2022.124537.

[5] Ruchi Gupta, Alejandro Pena-Bello, Kai Nino Streicher, Cattia Roduner, Yamshid Farhat, David Thöni, Martin Kumar Patel, and David Parra. Spatial analysis of distribution grid capacity and costs to enable massive deployment of PV, electric mobility and electric heating. *Applied Energy*, 287:116504, April 2021. ISSN 03062619. doi: 10.1016/j.apenergy.2021.116504.

[6] Christina Protopapadaki and Dirk Saelens. Heat pump and PV impact on residential low-voltage distribution grids as a function of building and district properties. *Applied Energy*, 192:268–281, April 2017. ISSN 03062619. doi: 10.1016/j.apenergy.2016.11.103.

[7] Fabian Wüllhorst, Sebastian Schwarz, Nico Fuchs, Laura Maier, Antonello Monti, and Dirk Müller. Impact of hybrid heat pump shares and building envelope retrofit rates on load penetration in German low-voltage grids. *Applied Energy*, 388:125530, June 2025. ISSN 03062619. doi: 10.1016/j.apenergy.2025.125530.

[8] Simon Meunier, Christina Protopapadaki, Ruben Baetens, and Dirk Saelens. Impact of residential low-carbon technologies on low-voltage grid reinforcements. *Applied Energy*, 297:117057, September 2021. ISSN 03062619. doi: 10.1016/j.apenergy.2021.117057.

[9] Muhammad Bashar Anwar, Matteo Muratori, Paige Jadun, Elaine Hale, Brian Bush, Paul Denholm, Ookie Ma, and Kara Podkaminer. Assessing the value of electric vehicle managed charging: a review of methodologies and results. *Energy Environ. Sci.*, 15:466–498, 2022. doi: 10.1039/D1EE02206G.

[10] Axel Ensslen, Philipp Ringler, Lasse Dörr, Patrick Jochem, Florian Zimmermann, and Wolf Fichtner. Incentivizing smart charging: Modeling charging tariffs for electric vehicles in German and French electricity markets. *Energy Research & Social Science*, 42:112–126, August 2018. ISSN 22146296. doi: 10.1016/j.erss.2018.02.013.

[11] Fei Teng, Zhaohao Ding, Zechun Hu, and Piampoom Sarikprueck. Technical review on advanced approaches for electric vehicle charging demand management, part i: Applications in electric power market and renewable energy integration. *IEEE Transactions on Industry Applications*, 56(5):5684–5694, 2020. doi: 10.1109/TIA.2020.2993991.

[12] Enxin Yao, Vincent W. S. Wong, and Robert Schober. Robust Frequency Regulation Capacity Scheduling Algorithm for Electric Vehicles. *IEEE Transactions on Smart Grid*, pages 1–14, 2016. ISSN 1949-3053, 1949-3061. doi: 10.1109/TSG.2016.2530660.

[13] Ge Chen, Nima Rashgi Shishvan, Zhaomiao Guo, and Junjie Qin. Quantifying spatiotemporal charging flexibility of electric vehicles as virtual grid assets to accelerate sustainable energy transition. *Cell Reports Physical Science*, 6(11):102905, 2025. ISSN 26663864. doi: 10.1016/j.xcrp.2025.102905.

[14] Lukas Franken, Andy Hackett, Jesus Lizana, Iegor Riepin, Ryan Jenkinson, Andrew Lyden, Lucy Yu, and Daniel Friedrich. Power system benefits of simultaneous domestic transport and heating demand flexibility in Great Britain's energy transition. *Applied Energy*, 377:124522, January 2025. ISSN 03062619. doi: 10.1016/j.apenergy.2024.124522.

[15] Trine Krogh Kristoffersen, Karsten Capion, and Peter Meibom. Optimal charging of electric drive vehicles in a market environment. *Applied Energy*, 88(5):1940–1948, 2011. ISSN 03062619. doi: 10.1016/j.apenergy.2010.12.015.

[16] Julia K. Szinai, Colin J.R. Sheppard, Nikit Abhyankar, and Anand R. Gopal. Reduced grid operating costs and renewable energy curtailment with electric vehicle charge management. *Energy Policy*, 136: 111051, 2020. ISSN 03014215. doi: 10.1016/j.enpol.2019.111051.

[17] Pranjal Barman, Lachit Dutta, Sushanta Bordoloi, Anamika Kalita, Pronamika Buragohain, Swapna Bharali, and Brian Azzopardi. Renewable energy integration with electric vehicle technology: A review of the existing smart charging approaches. *Renewable and Sustainable Energy Reviews*, 183:113518, 2023. ISSN 13640321. doi: 10.1016/j.rser.2023.113518.

[18] Reza Fachrizal, Mahmoud Shepero, Dennis Van Der Meer, Joakim Munkhammar, and Joakim Widén. Smart charging of electric vehicles considering photovoltaic power production and electricity consumption: A review. *eTransportation*, 4:100056, 2020. ISSN 25901168. doi: 10.1016/j.etran.2020.100056.

[19] Sachin Chandrashekar, Yixian Liu, and Ramteen Sioshansi. Wind-integration benefits of controlled plug-in electric vehicle charging. *Journal of Modern Power Systems and Clean Energy*, 5 (5):746–756, 2017. ISSN 2196-5625, 2196-5420. doi: 10.1007/s40565-017-0296-x.

[20] Philipp Mascherbauer, Miguel Martínez, Carlos Mateo, Songmin Yu, and Lukas Kranzl. Analyzing the impact of heating electrification and prosumaging on the future distribution grid costs. *Applied Energy*, 387:125563, June 2025. ISSN 03062619. doi: 10.1016/j.apenergy.2025.125563.

[21] Matteo Muratori, Vittorio Marano, Ramteen Sioshansi, and Giorgio Rizzoni. Energy consumption of residential hvac systems: a simple physically-based model. In *2012 IEEE Power and Energy Society General Meeting*, San Diego, CA, USA, July 2012. IEEE. 22–26 July 2012.

[22] Matteo Muratori, Margaret C. Roberts, Ramteen Sioshansi, Vittorio Marano, and Giorgio Rizzoni. A highly resolved modeling technique to simulate residential power demand. *Applied Energy*, 107:465–473, 2013. doi: 10.1016/j.apenergy.2013.02.057.

[23] Tjarko Tjaden, Joseph Bergner, Johannes Weniger, and Volker Quaschning. Repräsentative elektrische lastprofile für wohngebäude in deutschland auf 1-sekündiger datenbasis [Representative electrical load profiles for single-family houses in germany based on 1-second data], 2015. URL https://solar.htw-berlin.de/elektrische-lastprofile-fuer-wohngebaeude. Available online.

[24] California Energy Commission. California plug-in electric vehicle infrastructure projections: 2017–2025. future infrastructure needs for reaching the state's zero-emission-vehicle deployment goal, 2018. URL https://www.nrel.gov/docs/fy18osti/70893.pdf. Accessed: 2023-10-09.

[25] Axel Ensslen, Christian Will, and Patrick Jochem. Simulating Electric Vehicle Diffusion and Charging Activities in France and Germany. *World Electric Vehicle Journal*, 10(4):73, November 2019. ISSN 2032-6653. doi: 10.3390/wevj10040073.

[26] Tien Linh Cao Van, Lukas Barthelmes, Till Gnann, Daniel Speth, and Martin Kagerbauer. Enhancing electric vehicle market diffusion modeling: A German case study on environmental policy integration. *Energy Strategy Reviews*, 50:101244, November 2023. ISSN 2211467X. doi: 10.1016/j.esr.2023.101244.

[27] Lorenzo Sica, Angela Carboni, Francesco Paolo Deflorio, Filippo Fappanni, and Cristiana Botta. User Adoption of Electrified Powertrains: Identification of Factors Through Discrete Choice Modelling. *Future Transportation*, 5(1):16, February 2025. ISSN 2673-7590. doi: 10.3390/futuretransp5010016.

[28] Fabian Arnold, Arne Lilienkamp, and Nils Namockel. Diffusion of electric vehicles and their flexibility potential for smoothing residual demand — A spatio-temporal analysis for Germany. *Energy*, 308: 132619, November 2024. ISSN 03605442. doi: 10.1016/j.energy.2024.132619.

[29] Phillip Paevere, Andrew Higgins, Zhengen Ren, Mark Horn, George Grozev, and Cheryl McNamara. Spatio-temporal modelling of electric vehicle charging demand and impacts on peak household electrical load. *Sustainability Science*, 9(1):61–76, January 2014. ISSN 1862-4065, 1862-4057. doi: 10.1007/s11625-013-0235-3.

[30] Fabian Heymann, Carlos Pereira, Vladimiro Miranda, and Filipe Joel Soares. Spatial load forecasting of electric vehicle charging using GIS and diffusion theory. In *2017 IEEE PES Innovative Smart Grid Technologies Conference Europe (ISGT-Europe)*, pages 1–6, Torino, September 2017. IEEE. ISBN 978-1-5386-1953-7. doi: 10.1109/ISGTEurope.2017.8260172.

[31] Mingyue Selena Sheng, Le Wen, Basil Sharp, Bo Du, Prakash Ranjitkar, and Douglas Wilson. A spatio-temporal approach to electric vehicle uptake: Evidence from New Zealand. *Transportation Research Part D: Transport and Environment*, 105:103256, April 2022. ISSN 13619209. doi: 10.1016/j.trd.2022.103256.

[32] Beneharo Reveron Baecker, Soner Candas, Deniz Tepe, and Anurag Mohapatra. Generation of low-voltage synthetic grid data for energy system modeling with the pylovo tool. *Sustainable Energy, Grids and Networks*, 41:101617, March 2025. ISSN 23524677. doi: 10.1016/j.segan.2024.101617.

[33] Soner Candas, Beneharo Reveron Baecker, Anurag Mohapatra, and Thomas Hamacher. Optimization-based framework for low-voltage grid reinforcement assessment under various levels of flexibility and coordination. *Applied Energy*, 343:121147, August 2023. ISSN 03062619. doi: 10.1016/j.apenergy.2023.121147.

[34] Sheridan Few, Predrag Djapic, Goran Strbac, Jenny Nelson, and Chiara Candelise. A geographically disaggregated approach to

integrate low-carbon technologies across local electricity networks. *Nature Energy*, 9(7):871–882, May 2024. ISSN 2058-7546. doi: 10.1038/s41560-024-01542-6.

[35] Fabian Heymann, Frederik vom Scheidt, Filipe J. Soares, Pablo Duenas, and Vladimiro Miranda. Forecasting Energy Technology Diffusion in Space and Time: Model Design, Parameter Choice and Calibration. *IEEE Transactions on Sustainable Energy*, 12(2): 802–809, April 2021. ISSN 1949-3037. doi: 10.1109/TSTE.2020.3020426.

[36] Scott A. Robinson and Varun Rai. Determinants of spatio-temporal patterns of energy technology adoption: An agent-based modeling approach. *Applied Energy*, 151:273–284, August 2015. ISSN 03062619. doi: 10.1016/j.apenergy.2015.04.071.

[37] Minhyun Lee and Taehoon Hong. Hybrid agent-based modeling of rooftop solar photovoltaic adoption by integrating the geographic information system and data mining technique. *Energy Conversion and Management*, 183:266–279, March 2019. ISSN 01968904. doi: 10.1016/j.enconman.2018.12.096.

[38] Ali Alderete Peralta, Nazmiye Balta-Ozkan, and Philip Longhurst. Spatio-temporal modelling of solar photovoltaic adoption: An integrated neural networks and agent-based modelling approach. *Applied Energy*, 305:117949, January 2022. ISSN 03062619. doi: 10.1016/j.apenergy.2021.117949.

[39] Zahra Radhi A. Salman and Nooreya Sayed Shehab. Spatial-Temporal Machine Learning Analysis of Solar PV Adoption: Uncovering Threshold Effects. In *2025 5th International Conference on Sustainable Islamic Business and Finance (SIBF)*, pages 1–5, December 2025. doi: 10.1109/SIBF68061.2025.11455316.

[40] Giacomo Falchetta, Enrica De Cian, Filippo Pavanello, and Ian Sue Wing. Inequalities in global residential cooling energy use to 2050. *Nature Communications*, 15(1):7874, September 2024. ISSN 2041-1723. doi: 10.1038/s41467-024-52028-8.

[41] Vassilis Daioglou, Bas J. Van Ruijven, and Detlef P. Van Vuuren. Model projections for household energy use in developing countries. *Energy*, 37(1):601–615, January 2012. ISSN 03605442. doi: 10.1016/j.energy.2011.10.044.

[42] Enrica De Cian, Giacomo Falchetta, Filippo Pavanello, Yasmin Romitti, and Ian Sue Wing. The impact of air conditioning on residential electricity consumption across world countries. *Journal of Environmental Economics and Management*, 131:103122, May 2025. ISSN 00950696. doi: 10.1016/j.jeem.2025.103122.

[43] Marijn J. Ton, Michiel W. Ingels, Jens A. De Bruijn, Hans De Moel, Lena Reimann, Wouter J. W. Botzen, and Jeroen C. J. H. Aerts. A global dataset of 7 billion individuals with socio-economic characteristics. *Scientific Data*, 11(1):1096, October 2024. ISSN 2052-4463. doi: 10.1038/s41597-024-03864-2.

[44] Lijun Sun, Alexander Erath, and Ming Cai. A hierarchical mixture modeling framework for population synthesis. *Transportation Research Part B: Methodological*, 114:199–212, August 2018. ISSN 01912615. doi: 10.1016/j.trb.2018.06.002.

[45] Xin Ye, Karthik Konduri, Ram M Pendyala, Bhargava Sana, and Paul Waddell. A methodology to match distributions of both household and person attributes in the generation of synthetic populations. In *88th Annual Meeting of the transportation research Board, Washington, DC*, volume 36, 2009.

[46] Richard J. Beckman, Keith A. Baggerly, and Michael D. McKay. Creating synthetic baseline populations. *Transportation Research Part A: Policy and Practice*, 30(6):415–429, November 1996. ISSN 09658564. doi: 10.1016/0965-8564(96)00004-3.

[47] Karthik C. Konduri, Daehyun You, Venu M. Garikapati, and Ram M. Pendyala. Enhanced Synthetic Population Generator That Accommodates Control Variables at Multiple Geographic Resolutions. *Transportation Research Record: Journal of the Transportation Research Board*, 2563(1):40–50, January 2016. ISSN 0361-1981, 2169-4052. doi: 10.3141/2563-08.

[48] Ana Tsui Moreno and Rolf Moeckel. Population Synthesis Handling Three Geographical Resolutions. *ISPRS International Journal of Geo-Information*, 7(5):174, May 2018. ISSN 2220-9964. doi: 10.3390/ijgi7050174.

[49] Max Kleinebrahm, Jacopo Torriti, Russell McKenna, Armin Ardone, and Wolf Fichtner. Using neural networks to model long-term dependencies in occupancy behavior. *Energy and Buildings*, 240: 110879, June 2021. ISSN 03787788. doi: 10.1016/j.enbuild.2021.110879.

[50] Long Cheng, Jonas De Vos, Kunbo Shi, Min Yang, Xuewu Chen, and Frank Witlox. Do residential location effects on travel behavior differ between the elderly and younger adults? *Transportation Research Part D: Transport and Environment*, 73:367–380, August 2019. ISSN 13619209. doi: 10.1016/j.trd.2019.07.015.

[51] Donggen Wang and Meng Zhou. The built environment and travel behavior in urban China: A literature review. *Transportation Research Part D: Transport and Environment*, 52:574–585, May 2017. ISSN 13619209. doi: 10.1016/j.trd.2016.10.031.

[52] Jean-Philippe Antoni and Olivier Klein. Generating a Located Synthetic Population of Individuals, Households, and Dwellings. *SSRN Electronic Journal*, 2017. ISSN 1556-5068. doi: 10.2139/ssrn.2972615.

[53] Dana R. Thomson, Lieke Kools, and Warren C. Jochem. Linking synthetic populations to household geolocations: A demonstration in namibia. *Data*, 3(3), 2018. ISSN 2306-5729. doi: 10.3390/data3030030. URL https://www.mdpi.com/2306-5729/3/3/30.

[54] Patrick Plötz, Uta Schneider, Joachim Globisch, and Elisabeth Dütschke. Who will buy electric vehicles? Identifying early adopters in Germany. *Transportation Research Part A: Policy and Practice*, 67:96–109, September 2014. ISSN 09658564. doi: 10.1016/j.tra.2014.06.006.

[55] Alim Nayum, Christian A. Klöckner, and Mehmet Mehmetoglu. Comparison of socio-psychological characteristics of conventional and battery electric car buyers. *Travel Behaviour and Society*, 3:8–20, January 2016. ISSN 2214367X. doi: 10.1016/j.tbs.2015.03.005.

[56] Zhibin Chen, Wei Liu, and Yafeng Yin. Deployment of stationary and dynamic charging infrastructure for electric vehicles along traffic corridors. *Transportation Research Part C: Emerging Technologies*, 77:185–206, April 2017. ISSN 0968090X. doi: 10.1016/j.trc.2017.01.021.

[57] Rohan Best and Fatemeh Nazifi. Analyzing electric vehicle uptake based on actual household distributions: A contribution to empirical policy formulation. *Transport Policy*, 137:100–108, June 2023. ISSN 0967070X. doi: 10.1016/j.tranpol.2023.04.011.

[58] Elisabeth Fevang, Erik Figenbaum, Lasse Fridstrøm, Askill H. Halse, Karen E. Hauge, Bjørn G. Johansen, and Oddbjørn Raaum. Who goes electric? The anatomy of electric car ownership in Norway. *Transportation Research Part D: Transport and Environment*, 92:102727, March 2021. ISSN 13619209. doi: 10.1016/j.trd.2021.102727.

[59] Meiyu (Melrose) Pan, Majbah Uddin, and Hyeonsup Lim. Understanding electric vehicle ownership using data fusion and spatial modeling. *Transportation Research Part D: Transport and Environment*, 127:104075, February 2024. ISSN 13619209. doi: 10.1016/j.trd.2024.104075.

[60] Rajeev Ranjan Kumar and Kumar Alok. Adoption of electric vehicle: A literature review and prospects for sustainability. *Journal of Cleaner Production*, 253:119911, April 2020. ISSN 09596526. doi: 10.1016/j.jclepro.2019.119911.

[61] Forschungsdatenzentren der Statistischen Ämter des Bundes und der Länder. Mikrozensus 2022, scientific use file (suf) [Microcensus 2022, scientific use file (SUF)], 2023. URL https://doi.org/10.21242/12211.2022.00.00.3.1.0.

[62] Jan Goebel, Markus M. Grabka, Carsten Schröder, Sabine Zinn, Charlotte Bartels, Mattis Beckmannshagen, Andreas Franken, Martin Gerike, Florian Griese, Christoph Halbmeier, Selin Kara, Peter Krause, Elisabeth Liebau, Jana Nebelin, Marvin Petrenz, Sarah Satilmis, Rainer Siegers, Hans Walter Steinhauer, Felix Süttmann, Knut Wenzig, Jascha Dräger, Miriam Gauer, Yogam Tchokni, and Claudia Saalbach. Socio-economic panel (soep), data from 1984–2022 (soep-core, v39, eu edition), October 2024. URL https://doi.

org/10.5684/soep.core.v39eu. Collection period: 1984–2022.

[63] Jan Goebel, Markus M. Grabka, Stefan Liebig, Martin Kroh, David Richter, Carsten Schröder, and Jürgen Schupp. The german socio-economic panel (soep). *Jahrbücher für Nationalökonomie und Statistik*, 239(2):345–360, 2019. doi: doi:10.1515/jbnst-2018-0022. URL https://doi.org/10.1515/jbnst-2018-0022.

[64] Statistisches Bundesamt (Destatis). Zensus 2022: Publikationen [Census 2022: Publications], 2025. URL https://www.destatis.de/DE/Themen/Gesellschaft-Umwelt/Bevoelkerung/Zensus2022/_publikationen.html. Accessed 2026-02-27.

[65] Sebastian Hörl and Milos Balac. Synthetic population and travel demand for Paris and Île-de-France based on open and publicly available data. *Transportation Research Part C: Emerging Technologies*, 130:103291, September 2021. ISSN 0968090X. doi: 10.1016/j.trc.2021.103291.

[66] Robin Lovelace and Dimitris Ballas. 'Truncate, replicate, sample': A method for creating integer weights for spatial microsimulation. *Computers, Environment and Urban Systems*, 41:1–11, September 2013. ISSN 01989715. doi: 10.1016/j.compenvurbsys.2013.03.004.

[67] Frank M. Bass. A new product growth for model consumer durables. *Management Science*, 15(5):215–227, 1969. doi: 10.1287/mnsc.15.5.215.

[68] Dimitris Potoglou and Yusak O. Susilo. Comparison of Vehicle-Ownership Models. *Transportation Research Record: Journal of the Transportation Research Board*, 2076(1):97–105, January 2008. ISSN 0361-1981, 2169-4052. doi: 10.3141/2076-11.

[69] GeoBasis-DE / BKG. Geodaten des bundesamtes für kartographie und geodäsie [Geodata of the federal agency for cartography and geodesy], 2025. URL http://www.bkg.bund.de. Open Data Datenlizenz Deutschland – Namensnennung – Version 2.0.

[70] European Parliament and Council of the European Union. Directive 2007/2/EC of the European Parliament and of the Council of 14 March 2007 establishing an Infrastructure for Spatial Information in the European Community (INSPIRE), 2007. URL https://knowledge-base.inspire.ec.europa.eu/publications/directive-20072ec-european-parliament-and-council-14-march-2007-establishing-infrastructure-spatial_en. Accessed 2026-06-12.

[71] Pietro Florio, Panagiotis Politis, Katarzyna Krasnodębska, Johannes H. Uhl, Michele Melchiorri, Ana M. Martinez, Georgia Kakoulaki, Martino Pesaresi, and Thomas Kemper. GHS-OBAT: Global, open building attribute data reporting age, function, height and compactness at footprint level. *Data in Brief*, 61:111751, August 2025. ISSN 23523409. doi: 10.1016/j.dib.2025.111751.

[72] Xiao Xiang Zhu, Sining Chen, Fahong Zhang, Yilei Shi, and Yuanyuan Wang. GlobalBuildingAtlas: an open global and complete dataset of building polygons, heights and LoD1 3D models. *Earth System Science Data*, 17(12):6647–6668, December 2025. ISSN 1866-3516. doi: 10.5194/essd-17-6647-2025.

[73] Tobias Loga, Britta Stein, Nikolaus Diefenbach, and Rolf Born. *Deutsche Wohngebäudetypologie: Beispielhafte Maßnahmen zur Verbesserung der Energieeffizienz von typischen Wohngebäuden [German Residential Building Typology: Example Measures for Improving the Energy Efficiency of Typical Residential Buildings]*. Institut Wohnen und Umwelt (IWU), Darmstadt, Germany, 2., erweiterte auflage edition, 2015. ISBN 978-3-941140-47-9. Prepared within the EU projects TABULA and EPISCOPE.

[74] Kraftfahrt-Bundesamt (KBA). Bestand an kraftfahrzeugen und kraftfahrzeuganhängern nach zulassungsbezirken, 1. januar 2025 (fz 1) [Stock of motor vehicles and motor vehicle trailers by registration district, 1 january 2025 (FZ 1)], 2025. URL https://www.kba.de/DE/Statistik/Produktkatalog/produkte/Fahrzeuge/fz1_b_uebersicht.html. accessed: 2026-03-20.

[75] Robert Follmer. Mobilität in deutschland – mid kurzbericht [Mobility in germany]. Technical Report FE-Nr. VB600001, infas Institut für angewandte Sozialwissenschaft GmbH, Deutsches Zentrum für Luft- und Raumfahrt e.V. (DLR), IVT Research GmbH und infas 360 GmbH im Auftrag des Bundesministers für Digitales und Verkehr, Bonn, Berlin, 2025. URL https://www.mobilitaet-in-deutschland.de/pdf/MiD2023_Kurzbericht.pdf.

[76] Kraftfahrt-Bundesamt. Fahrzeugbestand am 1. Januar 2026 [The vehicle stock as of 1 january 2026]. Pressemitteilung Nr. 09/2026, 2026. URL https://www.kba.de/DE/Presse/Pressemitteilungen/Fahrzeugbestand/2026/pm09_fz_bestand_pm_komplett.html. Accessed 2026-06-12.

[77] Oak Ridge National Laboratory. 2022 National Household Travel Survey: Codebook. Online document, 2024. URL https://nhts.ornl.gov/assets/2022/doc/codebook.pdf. Accessed 2026-06-12.

[78] Kraftfahrt-Bundesamt. Bestand an kraftfahrzeugen und kraftfahrzeuganhängern nach bundesländern, fahrzeugarten und ausgewählten merkmalen, 1. januar 2025 (fz 27) [Stock of motor vehicles and motor vehicle trailers by federal states, vehicle types and selected characteristics, 1 january 2025 (FZ 27)], 2025. URL https://www.kba.de/DE/Statistik/Produktkatalog/produkte/Fahrzeuge/fz27_b_uebersicht.html. Accessed: 2026-05-12.

[79] Federal Institute for Research on Building, Urban Affairs, and Spatial Development. Stadt- und Gemeindetyp 2019 [Urban and municipal type 2019]. https://www.bbsr.bund.de/BBSR/DE/forschung/raumbeobachtung/Raumabgrenzungen/deutschland/gemeinden/StadtGemeindetyp/stadt-gemeindetyp-2019.csv?__blob=publicationFile&v=2, 2019. Accessed: 2026-05-19.

[80] Roxana J. Javid and Ali Nejat. A comprehensive model of regional electric vehicle adoption and penetration. *Transport Policy*, 54:30–42, February 2017. ISSN 0967070X. doi: 10.1016/j.tranpol.2016.11.003.

[81] Taekwan Yoon, Christopher R. Cherry, Megan S. Ryerson, and John E. Bell. Carsharing demand estimation and fleet simulation with EV adoption. *Journal of Cleaner Production*, 206:1051–1058, January 2019. ISSN 09596526. doi: 10.1016/j.jclepro.2018.09.124.

[82] Fatemeh Nazari, Abolfazl (Kouros) Mohammadian, and Thomas Stephens. Modeling electric vehicle adoption considering a latent travel pattern construct and charging infrastructure. *Transportation Research Part D: Transport and Environment*, 72:65–82, July 2019. ISSN 13619209. doi: 10.1016/j.trd.2019.04.010.

[83] Fatemeh Nazari, Abolfazl (Kouros) Mohammadian, and Thomas Stephens. Dynamic Household Vehicle Decision Modeling Considering Plug-In Electric Vehicles. *Transportation Research Record: Journal of the Transportation Research Board*, 2672(49):91–100, December 2018. ISSN 0361-1981, 2169-4052. doi: 10.1177/0361198118796925.

[84] Yan Liu and Cinzia Cirillo. A Generalized Dynamic Discrete Choice Model for Green Vehicle Adoption. *Transportation Research Procedia*, 23:868–886, 2017. ISSN 23521465. doi: 10.1016/j.trpro.2017.05.048.

[85] Fanchao Liao, Eric Molin, Harry Timmermans, and Bert Van Wee. Consumer preferences for business models in electric vehicle adoption. *Transport Policy*, 73:12–24, January 2019. ISSN 0967070X. doi: 10.1016/j.tranpol.2018.10.006.

[86] Brett Smith, Doina Olaru, Fakhra Jabeen, and Stephen Greaves. Electric vehicles adoption: Environmental enthusiast bias in discrete choice models. *Transportation Research Part D: Transport and Environment*, 51:290–303, March 2017. ISSN 13619209. doi: 10.1016/j.trd.2017.01.008.

[87] Fanglei Jin, Enjian Yao, and Kun An. Understanding customers' battery electric vehicle sharing adoption based on hybrid choice model. *Journal of Cleaner Production*, 258:120764, June 2020. ISSN 09596526. doi: 10.1016/j.jclepro.2020.120764.

[88] Lavan T. Burra, Mohammad B. Al-Khasawneh, and Cinzia Cirillo. Impact of charging infrastructure on electric vehicle adoption: A synthetic population approach. *Travel Behaviour and Society*, 37:100834, October 2024. ISSN 2214367X. doi: 10.1016/j.tbs.2024.100834.

[89] Daniel Speth, Till Gnann, Patrick Plötz, Martin Wietschel, and Jan George. Future regional distribution of electric vehicles in germany. In *Proceedings of the Electric Vehicle Symposium (EVS33), Portland, OR, USA*, pages 14–17, 2020.

[90] U.S. Census Bureau. American Community Survey Public Use Microdata Sample (ACS PUMS). Data source description, 2026. URL https://www.census.gov/programs-surveys/acs/microdata.html. Accessed 2026-05-27.

[91] U.S. Census Bureau. Current Population Survey: Annual Social and Economic Supplement (CPS ASEC). Data source description, 2026. URL https://www.census.gov/programs-surveys/cps/data/datasets.html. Accessed 2026-05-27.

[92] U.S. Census Bureau. Explore Census Data. Official U.S. Census Bureau data portal for census and survey tables, 2026. URL https://data.census.gov/. Accessed 2026-05-27.

[93] Office for National Statistics. Labour Force Survey. Survey information page, 2026. URL https://www.ons.gov.uk/surveys/informationforhouseholdsandindividuals/householdandindividualsurveys/labourforcesurvey. Accessed 2026-05-27.

[94] Office for National Statistics. Census. Official Census data and documentation portal, 2026. URL https://www.ons.gov.uk/census. Accessed 2026-05-27.

[95] Australian Bureau of Statistics. Microdata and TableBuilder: Income and Housing, Australia. Microdata access and documentation page, 2026. URL https://www.abs.gov.au/statistics/microdata-tablebuilder/available-microdata-tablebuilder/income-and-housing-australia. Accessed 2026-05-27.

[96] Australian Bureau of Statistics. Census DataPacks. Census data product, 2026. URL https://www.abs.gov.au/census/find-census-data/datapacks. Accessed 2026-05-27.

[97] National Institute of Statistics and Economic. Labour Force Survey 2025. Micro-data access page, 2025. URL https://www.insee.fr/en/metadonnees/source/operation/s2227/acces-micro-donnees. Accessed 2026-05-27.

[98] National Institute of Statistics and Economic. Population Census. Population census source description and statistical data portal, 2026. URL https://www.insee.fr/en/metadonnees/source/serie/s1321. Accessed 2026-05-27.

[99] Eurostat. EU Labour Force Survey Microdata. Microdata access and documentation page, 2026. URL https://ec.europa.eu/eurostat/web/microdata/public-microdata/labour-force-survey. Accessed 2026-05-27.

[100] Eurostat. Census Hub. European population and housing census data access portal, 2026. URL https://ec.europa.eu/CensusHub. Accessed 2026-05-27.

[101] IPUMS International. Harmonized International Census Data For Social Science and Health Research. International census and survey microdata infrastructure, 2026. URL https://international.ipums.org/. Accessed 2026-05-27.

[102] IPUMS IHGIS. International Historical Geographic Information System. International census summary tables and GIS boundary files, 2026. URL https://ihgis.ipums.org/. Accessed 2026-05-27.

[103] Luxembourg Income Study. Luxembourg Income Study Database. Harmonised cross-national household income microdata database, 2026. URL https://www.lisdatacenter.org/our-data/lis-database/. Accessed 2026-05-27.

[104] ICF. DHS Program Survey Updates. International household survey programme website, 2026. URL https://dhsprogram.com/. Accessed 2026-05-27.

[105] Federal Highway Administration. National Household Travel Survey 2022. Household travel survey microdata and documentation, 2022. URL https://nhts.ornl.gov/. Accessed 2026-05-27.

[106] Department for Transport. National Travel Survey: 2024. National statistics release and survey documentation, 2025. URL https://www.gov.uk/government/statistics/national-travel-survey-2024. Accessed 2026-05-27.

[107] Statistical Data and Studies Department. Detailed Results of the 2019 French National Travel Survey. Mobility survey microdata and documentation, 2021. URL https://www.statistiques.developpement-durable.gouv.fr/resultats-detailles-de-lenquete-mobilite-des-personnes-de-2019. Accessed 2026-05-27.

[108] KfW Research. KfW Energy Transition Barometer. Household survey and report series on energy transition technologies in Germany, 2026. URL https://www.kfw.de/About-KfW/KfW-Research/KfW-Energiewendebarometer.html. Accessed 2026-05-27.

[109] U.S. Energy Information Administration. 2024 RECS Survey Data. Residential Energy Consumption Survey microdata and documentation, 2026. URL https://www.eia.gov/consumption/residential/data/2024/index.php?view=microdata. Accessed 2026-05-27.

[110] Miguel Poblete-Cazenave and Shonali Pachauri. A model of energy poverty and access: Estimating household electricity demand and appliance ownership. *Energy Economics*, 98:105266, June 2021. ISSN 01409883. doi: 10.1016/j.eneco.2021.105266.

[111] Miguel Poblete-Cazenave, Shonali Pachauri, Edward Byers, Alessio Mastrucci, and Bas van Ruijven. Global scenarios of household access to modern energy services under climate mitigation policy. *Nature Energy*, 6(8):824–833, August 2021. ISSN 2058-7546. doi: 10.1038/s41560-021-00871-0.

[112] Minda Ma, Shufan Zhang, Junhong Liu, Ran Yan, Weiguang Cai, Nan Zhou, and Jinyue Yan. Building floorspace and stock measurement: A review of global efforts, knowledge gaps, and research priorities. *Nexus*, 2(3):100075, September 2025. ISSN 29501601. doi: 10.1016/j.ynexs.2025.100075.

[113] Nikola Milojevic-Dupont, Felix Wagner, Florian Nachtigall, Jiawei Hu, Geza Boi Brüser, Marius Zumwald, Filip Biljecki, Niko Heeren, Lynn H. Kaack, Peter-Paul Pichler, and Felix Creutzig. EUBUCCO v0.1: European building stock characteristics in a common and open database for 200+ million individual buildings. *Scientific Data*, 10(1):147, March 2023. ISSN 2052-4463. doi: 10.1038/s41597-023-02040-2.

[114] Ralf Münnich, Rainer Schnell, Hanna Brenzel, Hannah Diekmann, Sebastian Dräger, Janna Emmenegger, Philip Höcker, Johannes Kopp, Hariolf Merkle, Kristina Neufang, Monika Obersneider, Julian Reinhold, Jannik Schaller, Simon Schmaus, and Petra Stein. A Population Based Regional Dynamic Microsimulation of Germany: The MikroSim Model. *methods*, data:23 Pages, April 2021. doi: 10.12758/MDA.2021.03.

[115] Steffen Maretzke, Jana Hoymann, and Claus Schlömer. Bevölkerungsprognose: Raumordnungsprognose 2045 [Spatial planning forecast 2045: Population forecast]. Technical Report 04/2024, Bundesinstitut für Bau-, Stadt- und Raumforschung, Bonn, 2024.

[116] Cathal O'Donoghue and Gijs Dekkers. Increasing the Impact of Dynamic Microsimulation Modelling. *International Journal of Microsimulation*, 11(1):61–96, 2017. doi: 10.34196/ijm.00174.

[117] Pauline Pohl, Philip Slepecki, and Martin Spielauer. STATSIM: Statistics Austria's dynamic microsimulation model for official population projections. *Statistical Journal of the IAOS: Journal of the International Association for Official Statistics*, 40(4):969–984, November 2024. ISSN 1874-7655, 1875-9254. doi: 10.1177/18747655241308058.

[118] Rolf Moeckel. Constraints in household relocation: Modeling land-use/transport interactions that respect time and monetary budgets. *Journal of Transport and Land Use*, January 2016. ISSN 1938-7849. doi: 10.5198/jtlu.2015.810.

[119] Paul Waddell, Alan Borning, Michael Noth, Nathan Freier, Michael Becke, and Gudmundur Ulfarsson. Microsimulation of urban development and location choices: Design and implementation of urbansim. *Networks and Spatial Economics*, 3:43–67, 2003.

[120] Moritz Raab, Jonathan Vogl, Tim Signer, and Max Kleinebrahm. Integration of electric vehicles into energy system models: A review. *Renewable and Sustainable Energy Reviews*, 238:117078, 2026. ISSN 1364-0321. doi: https://doi.org/10.1016/j.rser.2026.117078.

[121] Iain Staffell, Stefan Pfenninger, and Nathan Johnson. A global model of hourly space heating and cooling demand at multiple spatial scales. *Nature Energy*, 8(12):1328–1344, September 2023. ISSN 2058-7546. doi: 10.1038/s41560-023-01341-5.

Table 5
Main input parameters used in the case study.

Model component	Parameter	Value	Description
Synthetic population	ϵ	10^{-4}	IPU improvement threshold
Household-to-building matching	h_{story}	3.0 m	Average story height [73]
	ω	1	Unused-area penalty weight
	β	1000	Unassigned-household penalty weight
	λ_{type}	100	Building-type penalty weight
	λ_{age}	1	Building-age penalty weight
Vehicle ownership	δ	0.25	Conditional continuation probability for households with more than three vehicles
EV diffusion	M	49,339,166	Market potential, based on current vehicle stock [74]

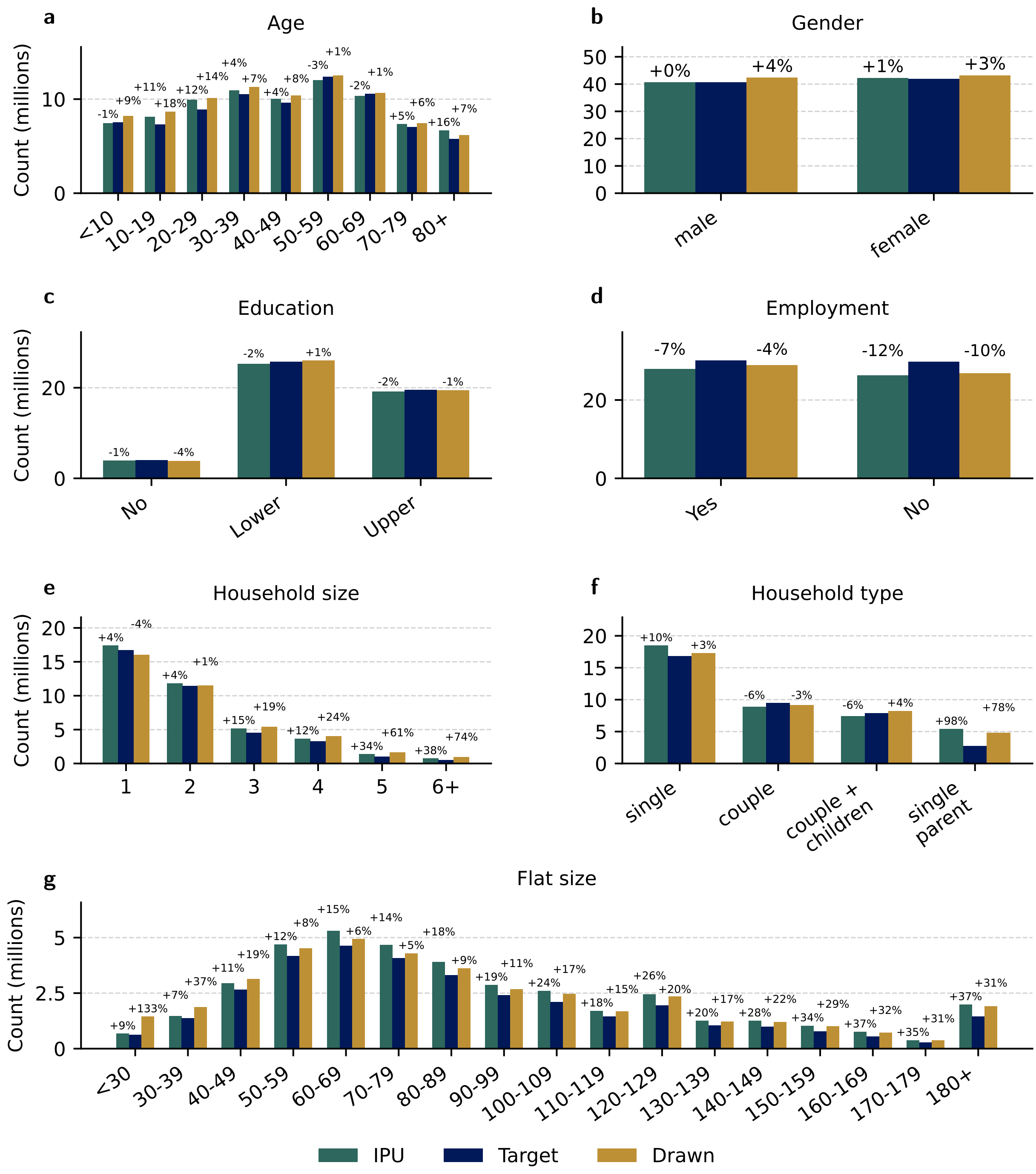

Fig. 6: Validation of the synthetic population against Census target marginals. Aggregated counts for Germany obtained from the Iterative Proportional Updating (IPU) weights and after household sampling (Drawn) are compared with the target counts from the marginal distributions (Target). Shown are all variables used as IPU constraints: age in years (**a**), gender (**b**), education (**c**), employment status (**d**), household size (**e**), household type (**f**), and flat size in m^2 (**g**). Relative deviations above the bars indicate the percentage difference between the IPU or Drawn counts and the corresponding target counts.

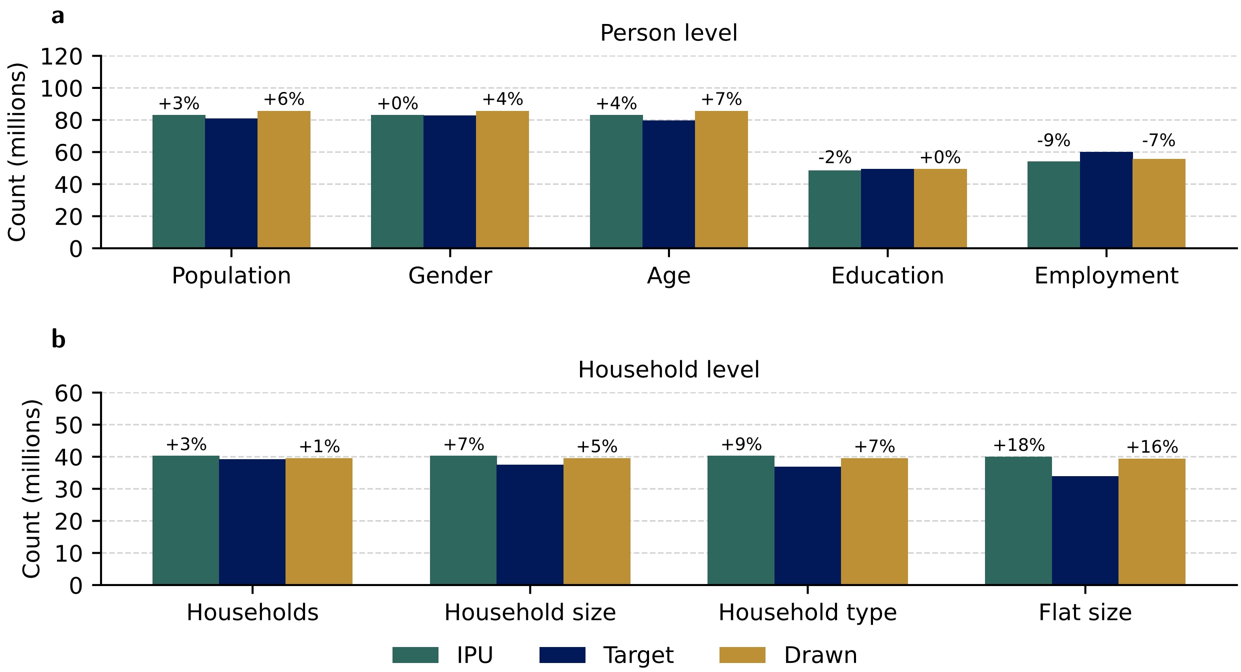

Fig. 7: Comparison of aggregated target and synthetic population counts for Germany. Counts obtained from the Iterative Proportional Updating (IPU) weights and after household sampling (Drawn) are compared with the target counts from the marginal distributions (Target). The comparison is shown for person-level totals, including the total population and the aggregated counts for age, gender, education, and employment status (**a**), and for household-level totals, including the total number of households and the aggregated counts for household size, household type, and living area (**b**). Relative deviations above the bars indicate the percentage difference between the IPU or Drawn counts and the corresponding target counts.

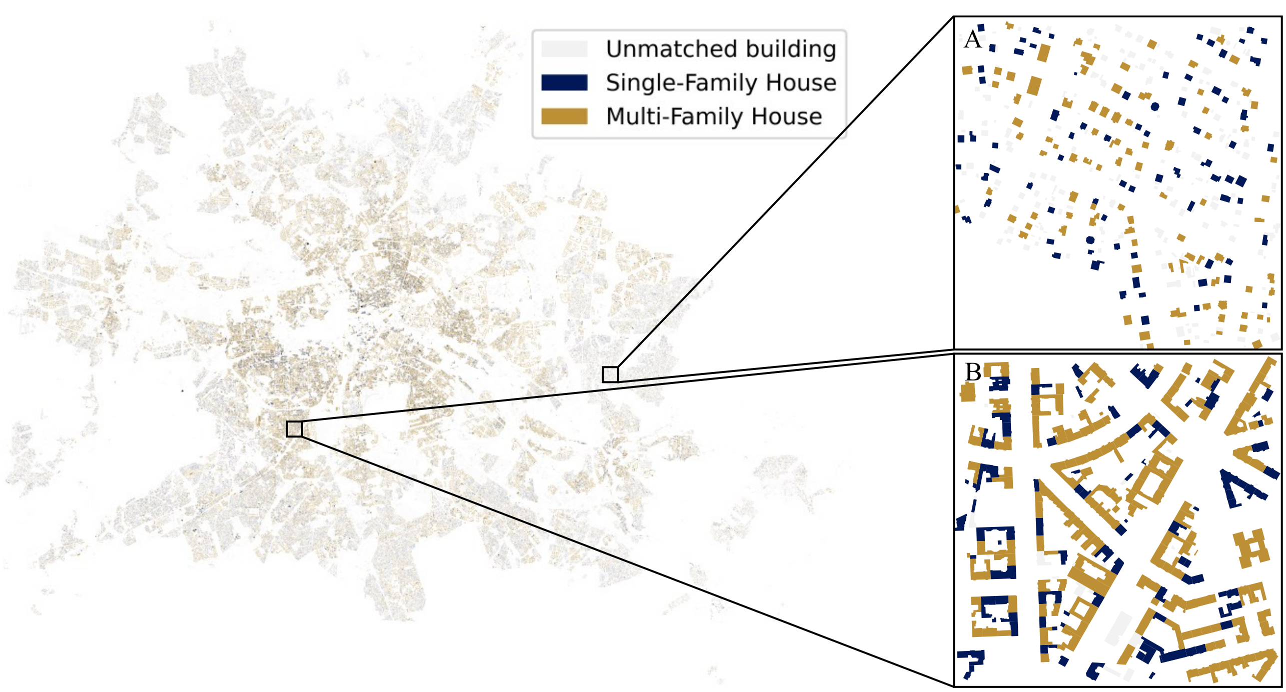

Fig. 8: Residential building classification in Berlin after household-to-building matching. Residential buildings are classified as unmatched, single-family houses, or multi-family houses based on the matching outcome. The full Berlin case is shown together with two selected 500×500 m grid cells, labeled A and B, corresponding to the grid cells shown in Fig. 4c. Compared with grid cell B, grid cell A has an approximately 31% higher average net household income and a substantially higher single-family house share, 25% compared with 4%. Average age is similar in both grid cells, at 44 years in grid cell A and 42 years in grid cell B.

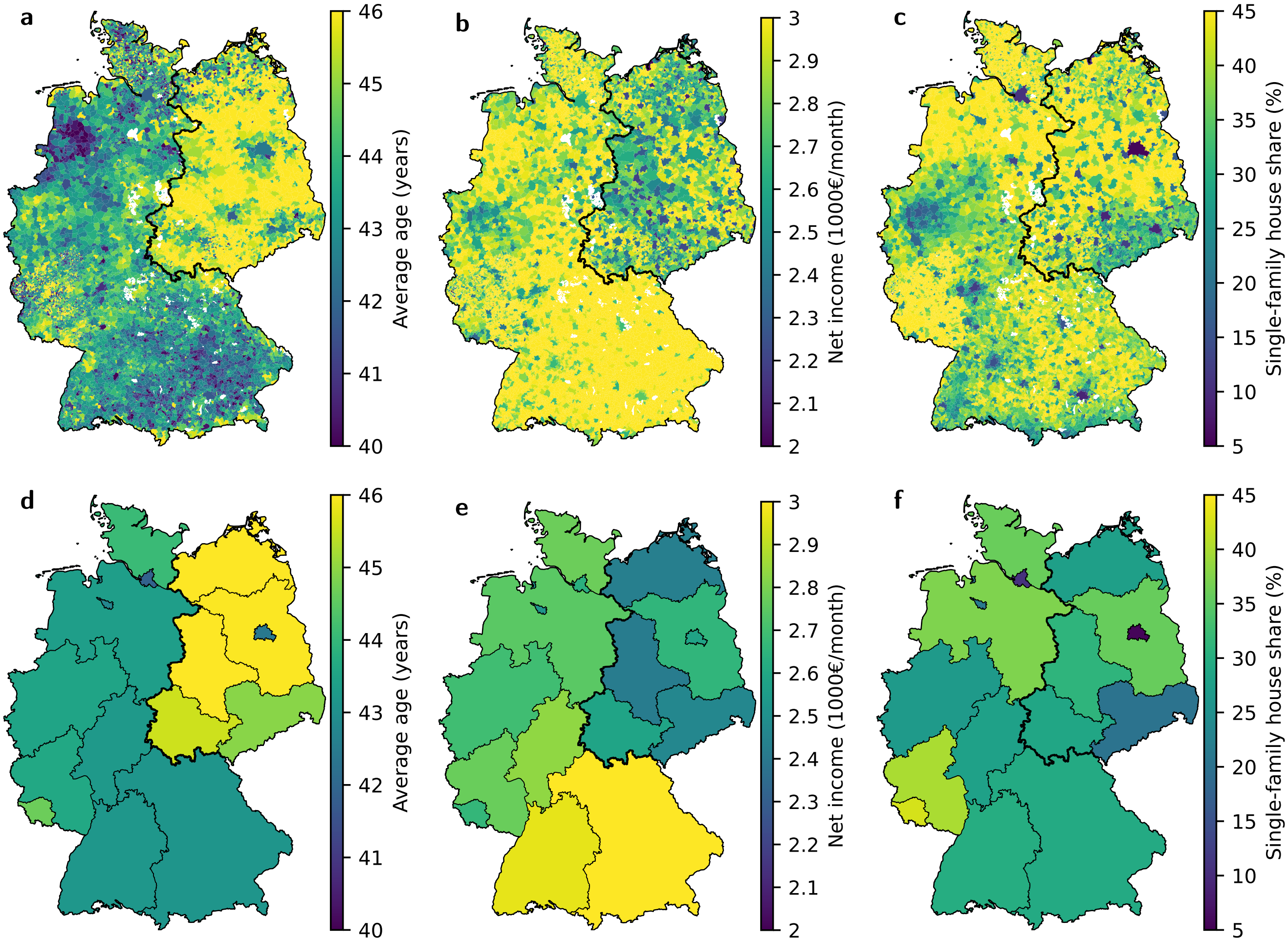

Fig. 9: Spatial distribution of key electric vehicle adoption determinants in East and West Germany. The municipal-level distributions of age (**a**), net household income (**b**), and single-family house share (**c**) are shown for the synthetic population. The corresponding average values are additionally aggregated to the federal-state level for the same determinants (**d–f**).

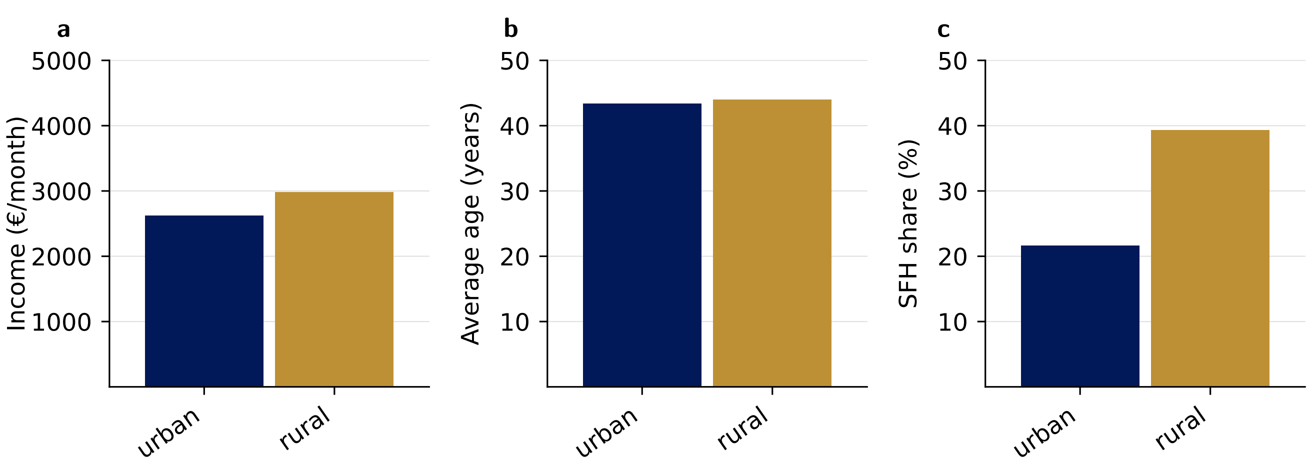

Fig. 10: Urban–rural differences in key electric vehicle adoption determinants. Bars show the mean values calculated separately across all municipalities classified as urban and all municipalities classified as rural. The comparison includes net household income (**a**), age (**b**), and single-family house share (**c**).

Table 6
Training and evaluation summary of the car ownership model.

Measure	Value
Sample composition	
Households	218,101
Households dropped due to missing building type	8,317
Households dropped due to missing vehicle ownership status	281
Households used for model estimation	209,503
Ownership class distribution, unweighted	
Households with zero vehicles	27,401
Households with one vehicle	99,883
Households with two vehicles	66,561
Households with three or more vehicles	15,658
Ownership class distribution, weighted	
Households with zero vehicles	40,353
Households with one vehicle	105,919
Households with two vehicles	49,156
Households with three or more vehicles	8,791
Training fit (80% split)	
McFadden pseudo-R^2	0.266
Adjusted McFadden pseudo-R^2	0.266
Test-set predictive performance (20% split)	
Multiclass log loss	0.840
Accuracy	0.626
Precision, weighted average	0.625
Recall, weighted average	0.626
F1-score, weighted average	0.603

Table 7
Qualitative auxiliary regression results for the car ownership model by vehicle ownership class. The main car ownership model is estimated as a weighted multinomial logistic regression using scikit-learn for predictive purposes. Since this implementation does not provide coefficient-level standard errors or p-values for the weighted multinomial model, the reported directions and significance levels are derived from auxiliary one-vs-rest weighted logistic regression models. The results are used for qualitative interpretation only and should not be interpreted as exact inference for the multinomial model.

Feature	Zero vehicles	One vehicle	Two vehicles	Three or more vehicles
Constant	$+^{***}$	$+^{***}$	$-^{***}$	$-^{***}$
Household net income	$-^{***}$	$-^{***}$	$+^{***}$	$+^{***}$
Building type: single-family house	$-^{***}$	$+^{***}$	$+^{***}$	$+^{***}$
Household size	$-^{***}$	$-^{***}$	$+^{***}$	$+^{***}$
Age: 0–9 years	$-$	$+^{***}$	$-^{***}$	$-^{***}$
Age: 10–19 years	$+^{***}$	$+^{***}$	$-^{***}$	$-^{***}$
Age: 20–29 years	$+^{***}$	$-^{***}$	$-^{***}$	$+^{***}$
Age: 30–39 years	$+^{***}$	$-$	$+$	$-^{***}$
Age: 50–59 years	$-^{***}$	$-^{**}$	$-^{*}$	$+^{***}$
Age: 60–69 years	$-^{***}$	$+^{***}$	$+^{***}$	$+^{***}$
Age: 70–79 years	$-^{***}$	$+^{***}$	$-^{***}$	$+$
Age: 80+ years	$+^{***}$	$+^{***}$	$-^{***}$	$-^{***}$
Education: no degree	$+^{***}$	$-^{***}$	$+^{***}$	$-^{**}$
Education: lower level	$-^{***}$	$-^{***}$	$+^{***}$	$+^{***}$
Education: upper level	$-^{***}$	$-^{***}$	$+^{***}$	$+^{***}$
State: Baden-Württemberg	$-$	$-^{**}$	$+^{***}$	$-$
State: Bavaria	$-^{**}$	$-^{***}$	$+^{***}$	$+$
State: Berlin	$+^{***}$	$-^{***}$	$-^{***}$	$-^{***}$
State: Brandenburg	$-$	$-^{***}$	$+^{***}$	$+$
State: Bremen	$+^{***}$	$-^{***}$	$-^{***}$	$-^{**}$
State: Hamburg	$+^{***}$	$-^{***}$	$-^{***}$	$-^{***}$
State: Hesse	$+^{*}$	$-^{***}$	$+^{**}$	$-$
State: Lower Saxony	$+$	$-^{**}$	$+^{***}$	$+$
State: Mecklenburg-Vorpommern	$-$	$-$	$+^{**}$	$-^{***}$
State: North Rhine-Westphalia	$-$	$-^{***}$	$+^{***}$	$-$
State: Rhineland-Palatinate	$-^{**}$	$-^{***}$	$+^{***}$	$+^{*}$
State: Saarland	$-^{***}$	$-^{***}$	$+^{***}$	$+^{***}$
State: Saxony	$+$	$-^{***}$	$+^{***}$	$+$
State: Saxony-Anhalt	$-^{*}$	$-^{***}$	$+^{***}$	$-$
State: Thuringia	$-^{***}$	$-^{***}$	$+^{***}$	$+^{*}$

Age and education variables are measured at the household level and indicate the number of household members in the respective age or education category. The reference category for age is 40–49 years; the reference category for state is Schleswig-Holstein. Significance levels: $^{***}p < 0.001$, $^{**}p < 0.01$, $^{*}p < 0.05$.

A. Soft compatibility penalties in the household–building matching

Let $i \in I$ index households and $j \in J$ index buildings. The binary variable (x_{ij}) equals 1 if household i is assigned to building j, and 0 otherwise. The full objective function (Eq. 8) contains the unassigned-household penalty and the unused-area penalty and can additionally include soft compatibility terms, here for building type and building age.

A.1. Building type penalty

Each household has an expected residential building type (t_i), distinguishing single-family houses and multi-family houses. Since GHS-OBAT only identifies residential buildings and does not distinguish single-family houses and multi-family houses directly, the building-side type is inferred from the assignment itself. Buildings occupied by exactly one household are classified as single-family houses, whereas buildings occupied by two or more households are classified as multi-family houses.

For households with known expected type, a binary mismatch variable z_{ij} is introduced and linked to the assignment decision such that $z_{ij} = 1$ if household i is assigned to building j and the occupancy-based type of building j differs from the household's expected type.

The building-type contribution to the objective is therefore

$$\mathcal{L}_{\text{type}} = \lambda_{\text{type}} \sum_{i} \sum_{j} z_{ij}. \tag{17}$$

A.2. Building age penalty

Let $[a_i^H, b_i^H]$ denote the expected building age interval of household i and $[a_j^B, b_j^B]$ the building age interval of building j. The age penalty function is defined as

$$d_{ij}^{\text{age}} = \begin{cases} 0, & \text{if } [a_i^H, b_i^H] \cap [a_j^B, b_j^B] \neq \emptyset, \\ a_j^B - b_i^H, & \text{if } b_i^H < a_j^B, \\ a_i^H - b_j^B, & \text{if } b_j^B < a_i^H. \end{cases} \tag{18}$$

Thus, overlapping age intervals incur no penalty, whereas non-overlapping intervals are penalized in proportion to the smallest year gap between them. The building-age contribution to the objective is

$$\mathcal{L}_{\text{age}} = \lambda_{\text{age}} \sum_{i \in I} \sum_{j \in J} d_{ij}^{\text{age}} x_{ij}. \tag{19}$$

If either the household age or the building age is missing, no age penalty is applied for that household–building pair.

Working Paper Series in Production and Energy

recent issues

Impressum

Karlsruher Institut für Technologie

Institut für Industriebetriebslehre und Industrielle Produktion (IIP)
Deutsch-Französisches Institut für Umweltforschung (DFIU)

Hertzstr. 16
D-76187 Karlsruhe

KIT – Die Universität in der Helmholtz-Gemeinschaft

Working Paper Series in Production and Energy
No. 82, August 2026

ISSN 2196-7296

www.iip.kit.edu